Applied Thermal Engineering 271 (2025) 126315

Contents lists available at ScienceDirect

Applied Thermal Engineering

journal homepage: www.elsevier.com/locate/apthermeng

Research Paper

Experimental analysis of energy-saving and eco-friendly refrigeration system design with condensate water management

Buğra Şensoy [a,*], Mustafa Aktaş [b], Ahmet Aktaş [b], Yaren Güven [b], Burak Aktekeli [c], Süleyman Erten [d], Seyfi Şevik [e]

[a] Gazi University, Graduate School of Natural and Applied Sciences, Turkiye
[b] Gazi University, Faculty of Technology, Department of Energy Systems Engineering, Turkiye
[c] Bilecik Şeyh Edebali University, Osmaneli Vocational School, Worker Health and Safety, Turkiye
[d] Nurdil Refrigeration Inc., Turkiye
[e] Hitit University, Vocational School of Technical Sciences, Electrical and Energy, Turkiye

ARTICLE INFO

Keywords:
Refrigeration system
Plug-in refrigerator
Energy efficiency
Overflow pan
Control algorithm

ABSTRACT

In this study, a low-cost plug-in refrigeration system was developed for commercial-scale production. The design includes an innovative condensation pan, a humidification unit, and utilizes airflow techniques. The system operates with environmentally friendly R290 refrigerant and features a specially developed control system that ensures seamless coordination among its components. In this study, designs based on original defrost water removal methodologies were developed. Thus, it was aimed to enhance energy efficiency and sustainability by efficiently removing defrost water without overflow. For these purposes, the system was tested for four days in two modes (Mode-1: defrost water is removed by electrical resistance (PTC) and condenser waste heat, and Mode-2: PTC is not used, defrost water is transferred to the ultrasonic humidifier by water pump). For both modes, the cold room was kept at two different relative humidity ranges (90–95 % and 100 %). Carbon emission reductions of up to 337.66 kg CO_2/m^2 and energy savings of up to 29.52 % were obtained in the system to reduce the PTC running time with Mode 2. The refrigeration process has been achieved for high performance, and a sustainable design was presented. The highest coefficient of performance (COP) and second law values of the system were calculated as 3.10 and 56.24 % on Day-3. The refrigeration process was realized with high performance, and a sustainable system with rational long-term results was created. Furthermore, this innovative design is feasible and has commercially preferable payback periods.

1. Introduction

Population growth in recent years, the trend towards improvement in living standards, the day-by-day increase in the number of supermarkets, and the demand for ready-to-eat and fresh food in the world have all led to the need for refrigerated food products. As a result of this need, energy consumption increases significantly in the areas where refrigerators are used heavily, especially in supermarkets. Approximately 3–4 % of the total electrical energy generated worldwide is used in supermarkets [1]. Supermarket refrigeration systems can be responsible for up to 60 % of the energy consumed throughout the supermarket [2]. In addition, refrigeration systems are responsible for 7.8 % of the world's greenhouse gas emissions [3]. Therefore, environmental concerns and sustainable living standards are frequently discussed. In this context, every improvement in energy efficiency and carbon emission reduction will contribute to sustainability.

In this regard, the literature has discussed studies on reducing carbon emissions and improving energy efficiency in refrigeration systems. Orlandi et al. [4] presented the energy consumption distributions in the refrigerator by simulation analysis in closed refrigerated display cabinets (RDC). They concluded that the gap between the doors should be reduced as much as possible to reduce thermal load and energy consumption. Yu and Chan [5] studied the optimization of condenser fan control for the coefficient of performance (COP) increase in refrigeration systems. Depending on the ambient and load conditions, it is determined that a COP increase of 11.4–237.2 % can be realized when the control mechanism works as desired. Tsamos et al. [6] conducted a study in which they compared a new generation design in which they used air-guiding fins on the front surface of open RDC shelves with a

* Corresponding author.
E-mail address: bugra.sensoy@gazi.edu.tr (B. Şensoy).

https://doi.org/10.1016/j.applthermaleng.2025.126315
Received 3 February 2025; Received in revised form 14 March 2025; Accepted 23 March 2025
Available online 26 March 2025

Nomenclature

Acronyms

AEC	Annual energy consumption
ASHP	Air source heat pump
COP	Coefficient of performance
DX-ASHP	Direct expansion solar-assisted heat pump
EEI	Energy efficiency index
ESRC	Ejector subcooling refrigeration cycle
GWP	Global warming potential
NTC	Negative temperature coefficient
ODP	Ozon depletion potential
PTC	Positive temperature coefficient
RDC	Refrigerated display cabinet
RH	Relative humidity (%)
SD	Secure digital
SMER	Specific moisture extraction rate (kg water/kWh)
SI	Sustainability index
T/RH	Temperature and relative humidity
VCRS	Vapor compression refrigeration system

Greek

η	Efficiency (%)
ϕ	Amount of CO_2 (kg CO_2/h)

Symbols

c	Specific heat capacity (kJ/kg K)
D_p	Depletion number
EC_{daily}	Daily energy consumption (kWh)
$\dot{E}x_y$	Exergy (kW)
H_w	Water level (m)
h	Enthalpy (kJ/kg)
h_m	Mass transfer coefficient (m/s)
i_1	System total current (A)
i_2	PTC resistance current (A)
i_3	Compressor motor current (A)
m	Mass (kg)
$\dot{m}$	Mass flow rate (kg/s)
P	Pressure (kPa)
$\dot{Q}_{cp}$	The heat transfer absorbed in the condensate pan (kW)
$\dot{Q}_{con}$	Condenser capacity (kW)
$\dot{Q}_e$	Evaporator capacity (kW)
$\overline{R}$	Gas constant (kJ/kg K)
R	Measured quantity
RH_1	Condenser outlet air relative humidity (%)
RH_2	Cold room air relative humidity (%)
RH_3	Outside air relative humidity (%)
s	Entropy (kJ/kg K)
Sh	Sherwood number
T	Temperature (K)
T_1	Evaporator inlet temperature (K)
T_2	Evaporator outlet temperature (K)
T_3	Evaporator surface temperature (K)
T_4	Compressor discharge (condensate pan inlet) temperature (K)
T_5	Compressor suction temperature (K)
T_6	Condenser inlet temperature (K)
T_7	Condenser outlet temperature (K)
T_8	PTC (overflow) pan water temperature (K)
T_9	Condensate pan water temperature (K)
T_{10}	Condenser outlet air temperature (K)
T_{11}	Cold room air temperature (K)
T_{12}	Outside air temperature (K)
t	Time (s)
v_{sys}	System voltage (V)
w	Error rates
W_R	Total uncertainty
$\dot{W}_{comp}$	Compressor power (kW)
$\dot{W}_{PTC}$	PTC power (kW)
x	Independent variables
Z	Enviroeconomic parameter ($)
z	International carbon price ($)

Subscripts

0	Dead state reference point
CO_2	Carbon dioxide
con	Condenser
comp	Compressor
comp,d	Compressor discharge
comp,s	Compressor suction
con,fan	Condenser fan
con,i	Condenser inlet
con,o	Condenser outlet
cp	Condensate pan
e	Evaporator
e,fan	Evaporator fan
e,i	Evaporator inlet
e,o	Evaporator outlet
ev	Expansion valve
is	Isentropic
mech	Mechanical
r	Refrigerant
tot	Total
II	Second

conventional design in a simulation environment. Thanks to this integration, approximately 60 % energy savings were achieved. Approximately 60 % energy savings were achieved with this configuration.

Ocak et al. [7] investigated the effect of compressor selection on energy consumption in RDCs. For this, they used two identical refrigeration systems with R290 refrigerant, one using a constant-speed compressor and the other using a variable-speed compressor. By changing the compressor selection, energy consumption decreased by 25.9 %, and RDC's energy label value increased from C to B. Patil [8] carried out studies on condenser design to improve the coefficient of performance in a refrigeration system. Using a micro-fin tube condenser instead of a U-tube condenser in the refrigeration system increased the refrigeration capacity by 10 % and the COP by 17 %. With the multi-flow air curtain system in the refrigerator, Demirpolat [9] obtained 20 % higher COP, 40 % lower energy consumption, and 60 % lower energy efficiency index (EEI) than the single air curtain system. Karyeyen et al. [10] investigated the energy performance of horizontal RDCs. The airfoil design achieved a more effective air curtain, increasing the efficiency of the air curtain and reducing the infiltration of ambient warm air into the cabinet. In this way, the refrigeration capacity of the refrigeration system was decreased by 3.82 % with the use of an airfoil. Cirera et al. [11] developed a load management system that optimizes stochastic load behavior in industrial refrigeration systems and makes data-driven predictions. As a result of the experimental study, the operating time of the compressors working in parallel with this method was reduced by 77 %, and 17 % of electrical energy was saved. Güven et al. [12] determined that the compressor, evaporator fan, condenser fan, electric resistor, and lighting units are the equipment that cause energy consumption in RDC, and they developed an algorithm to keep these parameters under control by determining the energy consumption values

of this equipment. Koşan et al. [13] developed an environmentally friendly design that increases the energy efficiency index value with a fan control technique in an industrial refrigeration system using R290 refrigerant. In the new control design, both evaporator and condenser fans were controlled, resulting in a 25.2 % reduction in energy consumption. In contrast, the energy efficiency label was raised from class E to class D.

Thiessen et al. [14] found that energy consumption was reduced by 21 % when 56 % of the area of the refrigerant was covered with vacuum insulation panels. Shaban et al. [15] conducted a study on energy and exergy efficiency in RDCs. Using a variable-speed compressor and an electronic expansion valve, energy efficiency was achieved by 32 %, and exergy destruction was reduced by 76 % compared to the conventional system. Rauss et al. [16] investigated the effect of lighting systems on energy consumption in RDCs. Jouhara et al. [17] developed a new design for open RDC shelves with straight heat pipe technology and investigated the impact of the design on energy consumption and food preservation conditions. With this innovative design, the energy consumption was reduced by around 12 %, homogenizing the temperature profile of products.

Deniz et al. [18] used the compressor discharge pipes and the stagnant water in the condensate pan to transfer the refrigerant as superheated vapor to the compressor outlet. Adding fins to the discharge pipes in the condensate pan increased the heat transfer by 3.347 times compared to the case without fins. In this way, the refrigerator's energy consumption was reduced, and the energy class E in the current system was increased to D class with the new design. Evans and Foster [19] stated that the electrical resistances need 1500 W − 2000 W of power per hour, depending on the size of the system, for evaporation of the water in the condensate pan.

Studies on the removal of defrost water were reviewed. Song et al. [20] investigated the effect of drainage disposal of water generated at the end of the defrosting process on system performance. As a result of the study, with the use of the drainage system, the defrost efficiency increased from 47.5 % to 57.6 %, while the total energy consumption decreased from 898.1 kJ to 727.5 kJ. Rahman and Jacobi [21] found that groove geometry significantly affects water retention. They observed a significant improvement in meltwater drainage on micro-grooved surfaces, with up to 70 % more condensate drained than on a flat base surface. Li et al. [22] investigated the self-drainage characteristics on an inclined superhydrophobic surface. For slope angles greater than 30°, freezing water can be completely drained on superhydrophobic surfaces. They found that the superhydrophobic surface has an excellent self-draining ability, which provides the possibility for the improvement of defrost efficiency.

Kim et al. [23] proposed a new louvered fin design to improve the performance of the heat exchanger drainage. Asymmetric louvered fins improved the drainage performance of the retention water, which increased the heat transfer rate. They found that the surface tension at the leading edge of the asymmetric fin was 11 % less than that of the symmetric fin, which led to the improved drainage performance of asymmetric fins. Bansal and Xie [24] developed a dynamic simulation model to predict the thermodynamic characteristics of the evaporation of defrosted water in a refrigerator. The model results showed that the evaporation of water can be increased by raising the water temperature and optimizing the air velocity over the water tray. Due to the natural airflow over the water tray up to 0.9 m/s, evaporation rates can increase significantly with a slight air movement. Zhou et al. [25] developed a design with perforated louvered fins that requires less fin material while improving drainage. The 18° and 24° angle designs have shown excellent performance, significantly improving drainage efficiency.

In addition, the effects of using ultrasonic humidifiers in refrigeration systems on system performance and food products were investigated in the literature. Delele et al. [26] investigated how adding a humidifier to the cold room affects the products and the system. During refrigeration, the humidifier was turned on for 1 min and off for 10 min, and compared to the system without a humidifier, the relative humidity increased by an average of 10.1 %, while the time required for refrigeration decreased by 15.8 %, and the weight loss of the products decreased by 1.13 %. Fabbri et al. [27] concluded that using ultrasonic humidifiers in the vegetable and fruit supply chain reduces potential product losses by more than 20 % compared to a conventional supply chain. It has also been reported that using humidifiers can prevent carbon emissions of 0.1 kg CO_2 equivalent per unit mass of products.

Brown et al. [28] investigated the effects of ultrasonic humidifier use on a refrigeration system. With the use of humidifiers in the refrigeration system, the refrigeration load increased from 3.4 kW to 3.8 kW, and the average compressor run time increased by 8 %. Tirawat et al. [29] examined the effects of humidification during refrigeration on the product quality of white asparagus. It was concluded that when refrigeration and humidification were carried out at the same time, the water loss of the product decreased by 14 %, and the product's color deteriorated after one day with only refrigeration and after three days with refrigeration and humidification.

Jhee and Lee [30] investigated the defrosting characteristics of a positive temperature coefficient (PTC) heating plate and compared them experimentally with those of a conventional electric heater. They found that when the PTC heating plate is used and the discharged water is completely melted, the characteristics of the water discharge rate with the defrosting time show a smooth oscillation pattern. The defrosting efficiency of the PTC heating plate was found to be about 75 %, which is about 25 % higher than that of the electric heater. Westhaeuser et al. [31] to compensate for the insufficient heating capacity from the heat pump in the vehicle when the heat pump is running or in defrost mode, they have installed a High Voltage-Positive Temperature Coefficient as an electric heater in the heating, ventilation, and air conditioning unit air path after the heater core. Steiner and Rieberer [32] installed a PTC heater in the air path downstream of the internal heat exchanger to provide the required heating performance during the defrosting process. By using resistance heating with PTC elements to meet the heat demand of electric vehicles, the cruising range is significantly reduced at low outside temperatures. Wang et al. [33] investigated the PTC behavior of low Curie point PTC materials under different component ratios. The adaptive temperature control capability and stability of low Curie point PTC material in anti-icing applications were experimentally verified.

In energy efficiency studies conducted for plug-in refrigeration systems, studies to generally increase compressor efficiency come to the forefront. More literature is needed regarding the PTC resistance behavior, which is the most energy-consuming equipment after the compressor in plug-in refrigerators, and the removal of defrost water from the environment. To fill this gap in the literature, a refrigeration system operating with propane (R290), an environmentally friendly refrigerant, is designed, tested, and analyzed. Different approaches, such as fan positioning, fabric use, and compressor discharge line routing, are applied to achieve the maximum possible vapor mass flow and low energy consumption by reducing the PTC's operating requirement. In addition, a water pump is integrated into the refrigeration system for this purpose.

The objectives of this study are as follows:

- Designing a new plug-in refrigeration system that utilizes condenser waste heat and heat from the compressor discharge line to remove the defrost water as soon as possible without overflowing into the surroundings,
- Reducing the use of PTC resistance during the removal of defrost water from the system,
- Integration of a new automation system into the refrigeration system that optimizes system components according to changing ambient conditions and contributes to energy efficiency,
- Investigation of reducing the amount of consumed energy of the refrigeration system by changing the working time behavior of the components,

- Contributing to sustainability by developing an environmentally friendly approach with low carbon emissions,
- Designing a system with a high energy performance value to remove end users from the risk of carbon tax,
- Create a refrigeration system with a high sustainability index (SI) value by achieving the most feasible environmental and thermodynamic results,
- Manufacturing a feasible and economically preferable system for end users.

In the process of removing condensate water from the surroundings in plug-in refrigerators, as stated in the existing studies in the literature, PTC resistance is used, which causes a lot of energy consumption in the system. In this study, different unique approaches unavailable in the literature are developed. First, the condensate water receives the waste heat that is extracted from the condenser. Thus, the operating time of the PTC is shortened by utilizing waste heat during the mass transfer process of removing the condensate water. As another method, an ultrasonic humidifier and water pump are integrated into the system to eliminate the need for PTC operation. Due to this design, in a much shorter time than the first method, the water pump transferred the condensate water from the overflow pan to the ultrasonic humidifier for reuse in the humidification process. Additionally, the humidification unit built into the system and the control algorithm created especially for this study optimize energy efficiency and food product safety owing to this study. With the developed innovative solutions, energy efficiency is achieved, and as a result, positive economic, environmental, and sustainability outputs are obtained and contributed to the literature. In addition, an innovative condensate pan is developed that reuses the condensate water. Thus, this study also contributed to science in terms of efficient and effective water use, which is of global importance. The main objectives of this study are shown in Fig. 1.

2. Theoretical analysis

This section first reveals the relationships between energy, exergy, and the environment; on the other hand, it presents the equations used to reduce the data. The equations that form the basis of the analyses carried out during the study are presented in tables, and the relationships between the concepts are also included. Table 1 presents the equations used in the thermodynamic analyses, especially the first and second law efficiencies of thermodynamics, the exergy destruction of the refrigeration system components, and the condensate pan's heat transfer efficiency.

Mass transfer occurs in the overflow pan. Mass transfer analysis is required to find the evaporation time in this direction. Table 2 shows the equations used in the mass transfer analysis.

Another important analysis is to determine the energy consumption of the refrigeration system; the related equations are presented in Table 3. In addition, the same table includes equations for carbon emission, enviroeconomic, and sustainability index analyses. Considering the environmental impact of refrigeration systems is important in reducing their carbon emissions. Besides this exergy, which plays a vital role in assessing and increasing the use of sustainable energy and technologies, it allows for evaluating efficiency, environmental impact, and sustainability. The relationships between environmental impact, sustainability, and exergy efficiency are expressed in the equations in Table 3.

The relationships between environmental impact, sustainability, and exergy efficiency are indirectly applied to energy systems. Costing the greenhouse gas emissions that cause global warming by setting a carbon price will enable countries and those responsible for this effect to reduce the amount of carbon emissions. For this reason, enviroeconomic analyses of the designs put forward are carried out to reduce the related costs, which the whole world finds as a risk, as much as possible. The economic analysis is based upon the price of CO_2 emissions into the environment, which is the most powerful mechanism to promote the deployment of renewable energy technologies that do not emit carbon into the atmosphere. Recently, one of the most important factors in environmental policy that offers more effective but expensive solutions is eco-economics. It provides creative analysis that shows the financial effects of environmental policy decisions that are based on the cost of CO_2 emissions. The environmental analysis provides information regarding the environmental harm caused by the refrigerants, while the enviroeconomic analysis displays the economic cost of this harm. The refrigerant's GWP rates are used to evaluate environmental and enviroeconomic assessments [45,46,47,48].

Since it is essential to recognize that the world's resources are limited, it is necessary to meet present needs while preserving the ability to meet the needs of future generations. Therefore, a sustainability index analysis is carried out to evaluate the long-term results of the design rationally.

The uncertainty of the measurement is determined using the uncertainty analysis method and is caused by errors in devices, experimental circumstances, environmental conditions, readings, and measurement sites. Therefore, uncertainty analysis is applied to see and correct the errors introduced by the tools and apparatus used in this experimental investigation. Uncertainty analysis is calculated as [53]:

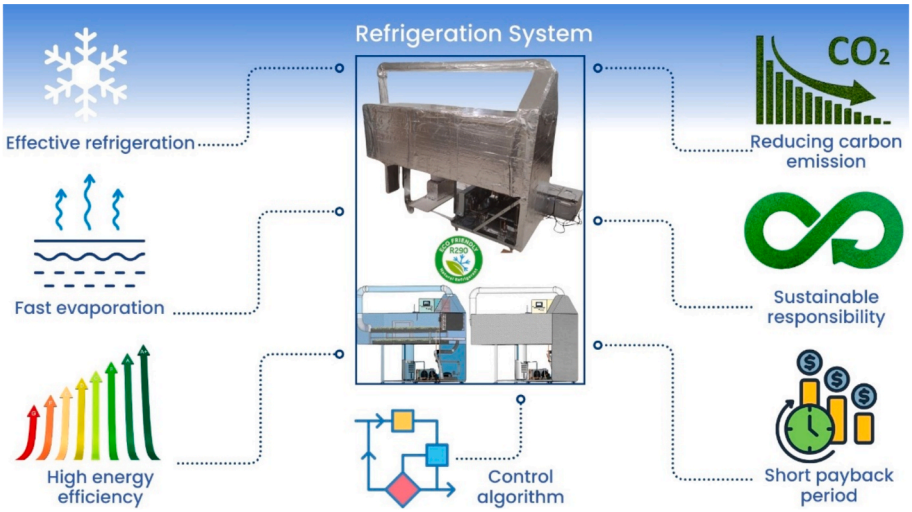

Fig. 1. The main objectives of this study.

Table 1
Thermodynamic analysis.

Parameters	Equations	Eqs. No	Refs. No.
Refrigerant mass flow rate	$\dot{m}_r = \frac{\dot{Q}_e}{(h_{e,o} - h_{e,i})}$	(1)	[34]
Evaporator capacity	$\dot{Q}_e = \dot{m}_r(h_{e,o} - h_{e,i})$	(2)	[35]
Evaporator exergy destruction	$\dot{E}x_{y,e} = \dot{m}_r\left[h_{e,i} - h_{e,o} - T_0\left(s_{e,i} - s_{e,o}\right)\right] - \left[-\dot{Q}_e\left(1 - \frac{T_0}{T_L}\right)\right]$	(3)	[36]
Compressor total efficiency	$\eta_{tot} = \eta_{is}.\eta_{mech} = \left(1 - 0.05\frac{P_{con}}{P_e}\right)\eta_{mech}$	(4)	[37]
Compressor power	$\dot{W}_{comp} = \frac{\dot{m}_r\left(h_{comp,d} - h_{comp,s}\right)}{\eta_{tot}}$	(5)	[38]
Compressor exergy destruction	$\dot{E}x_{y,comp} = \dot{W}_{comp,id} - \dot{m}_r\left[h_{comp,d} - h_{comp,s} - T_0\left(s_{comp,d} - s_{comp,s}\right)\right]$	(6)	[36]
Condenser capacity	$\dot{Q}_{con} = \dot{m}_r(h_{con,i} - h_{con,o})$	(7)	[35]
Condenser exergy destruction	$\dot{E}x_{y,con} = \dot{m}_r\left[h_{con,i} - h_{con,o} - T_0\left(s_{con,i} - s_{con,o}\right)\right] - \dot{Q}_{con}\left(1 - \frac{T_0}{T_H}\right)$	(8)	[36]
Expansion valve exergy destruction	$\dot{E}x_{y,ev} = \dot{m}_r\left[h_{con,o} - h_{evap,i} - T_0\left(s_{con,o} - s_{evap,i}\right)\right]$	(9)	[36]
Coefficient of performance	$\mathrm{COP} = \frac{\dot{m}_r\left(h_{e,o} - h_{e,i}\right)}{\dot{m}_r\left(h_{con,i} - h_{e,o}\right)}$	(10)	[39]
Total exergy destruction	$\dot{E}x_{y,tot} = \dot{E}x_{y,e} + \dot{E}x_{y,comp} + \dot{E}x_{y,con} + \dot{E}x_{y,ev}$	(11)	[36]
Second law efficiency	$\eta_{II} = 1 - \frac{\dot{E}x_{tot}}{\dot{W}_{comp,id}}$	(12)	[36]
Condensate pan efficiency	$\eta_{cp} = \frac{\dot{Q}_{cp}}{\dot{Q}_{con}} = \frac{\dot{m}_r c_r(T_4 - T_6)}{\dot{m}_r\left(h_{con,i} - h_{con,o}\right)}$	(13)	[40]

Table 2
Mass transfer analysis.

Parameters	Equations	Eqs. No.	Refs. No.
Sherwood number	$Sh = 0.037(Re^{0.8})Sc^{1/3}$	(14)	[41]
Coefficient of mass transfer	$h_m = \frac{Sh\ D_{AB}}{L}$	(15)	[42]
Mass transfer rate of vapor	$\dot{m}_{water} = \left(\frac{h_m}{\overline{R}T}\right)(P_d - P_b)$	(16)	[43]
Specific moisture extraction rate	$\mathrm{SMER} = \frac{m_{water}}{\dot{W}_{PTC}\ t_{PTC}}$	(17)	[44]

$$W_R = \left[\left(\frac{\delta R}{\partial x_1}w_1\right)^2 + \left(\frac{\delta R}{\partial x_2}w_2\right)^2 + \cdots + \left(\frac{\delta R}{\partial x_n}w_n\right)^2\right]^{1/2} \quad (24)$$

3. Material and method

This section consists of the subheadings of refrigeration system design, control algorithm structure, and experimental procedure. In this study, cold room conditions were created for mandarins. In this direction, when mandarins are not under appropriate refrigeration conditions, they lose their water, acid, and aroma, while color change, collapse, and decay occur in their external appearance due to the deterioration of their contents [54]. In this respect, the optimum values for temperature and relative humidity, the most important mandarin storage requirements, were investigated from the literature. In long-term storage, under 90–95 % relative humidity and 2–4 °C temperature values, weight loss, rot development, and physiological disorder appearance rates are minimal, taste is optimum, and internal quality parameters are found to be sufficient [55,56]. While these values constitute the optimum conditions of this study, storage conditions at 2–4 °C and 100 % relative humidity were determined as the extreme conditions of the study.

3.1. System design

Refrigeration systems are designed according to the mechanical vapor compression refrigeration cycle principle. Icing occurs on the evaporator surface during the relevant cycle, reducing the cycle efficiency. To solve this situation, the defrosting process eliminates the icing on the evaporator surface in the refrigeration cycle, and water is released by melting the ice. Plug-in refrigerators lack a drainage line, whereas central refrigeration systems include one to remove any water that may accumulate. In plug-in refrigerators, the water that occurs after defrosting is collected in the condensate pan. In the condensate pan, there is an electric resistance to water evaporation. As mentioned in the

Table 3
Analyzes of energy consumption, carbon emission, and sustainability.

Parameters	Equations	Eqs. No.	Refs. No.
Annual energy consumption	$\mathrm{AEC} = \mathrm{EC_{daily}}\ \mathrm{x}\ 365$	(18)	[49]
Daily energy consumption of the refrigeration system	$\mathrm{EC_{daily}} = \left[\left(\dot{W}_{comp}\ t_{comp}\right) + \left(\dot{W}_{e,fan}\ t_{e,fan}\right) + \left(\dot{W}_{con,fan}\ t_{con,fan}\right) + \left(\dot{W}_{PTC}\ t_{PTC}\right)\right]$	(19)	[49]
Carbon emission amount	$\phi_{CO_2} = 0.479\ \mathrm{kgCO_2/kWh\ x\ AEC}$	(20)	[50]
Enviroeconomic analysis	$Z_{CO_2} = \phi_{CO_2} x\ z_{CO_2}$	(21)	[51]
Depletion factor	$D_p = 1\text{-}\eta_{II}$	(22)	[52]
Sustainability index	$\mathrm{SI} = \frac{1}{D_p}$	(23)	[52]

previous section, the electric resistance effect seriously burdens the refrigeration system's electricity consumption. In addition, when the power of the electric resistance is insufficient, the defrost water overflows into the surrounding environment of the refrigeration systems.

Currently, the refrigeration industry expects to overcome the problem of high-energy consumption by minimizing the use of electric resistance and preventing the defrost water from overflowing into the surroundings. Therefore, this study proposes an alternative design to overcome these problems. With this alternative design, the compressor discharge line is passed through the condensate pan to evaporate the defrost water in the condensate pan, and antibacterial water absorption fabrics are specially arranged in the condensate pan. The condenser fans are placed as close to the condensate pan to blow hot air on the water surfaces inside the overflow pan. Then, to avoid the risk of water overflowing the surroundings, an overflow pan is created with a pipe coming out of the condensate pan, and an electric resistance is placed in this pan. In addition, with the various sensors placed in the system, the energy efficiency process is reinforced by monitoring the system with the created control algorithm.

Before installation, a 3D drawing was used to design the refrigeration system in detail. Fig. 2 displays the design's final perspective. The components corresponding to the numbers in Fig. 2 are explained under the figure title.

The discharge line from the compressor outlet to the condenser is first passed through the condensate pan. Then, the system continues to operate based on the vapor compression refrigeration cycle. The design also aims to use the maximum amount of fabric area possible to absorb as much water as possible in the condensate pan. In addition, the condenser fans are positioned as close as possible to the overflow pan so that the hot air reaches the water at the highest possible speed and temperature. Therefore, the design aims to achieve the maximum possible vapor mass flow to evaporate the water in the overflow pan quickly. By maximizing this flow, the operating requirement of the PTC is reduced. This results in lower energy consumption. This design is referred to as Mode-1 in this study. During the removal of the defrost water coming to the overflow pan in the refrigeration system, the PTC is not used at all, and this water is transferred with the help of a pump to be used in the ultrasonic humidifier in the system is referred to as Mode-2. Equipment, measuring instruments, and measuring points are given in Tables 4-5, while Mode-1 and Mode-2 are explained in detail in the

Table 4
The characteristics of equipment and features of the designed refrigeration system.

#	Equipment	Capacity	Qty.	Features
1	Compressor	736 W	1	Hermetic structure and −10 °C/ +45 °C operating temperature range.
2	Condenser	2250 W	1	Microchannel structure.
3	Condenser fans	250 m^3/h	2	With ECM technology and at 1400 rpm.
4	Evaporator	1500 W	1	20 pieces of 3/8″ diameter copper tubes and aluminum fins.
5	Evaporator fans	6 W	6	Withstand low operating temperature and runs 2300 rpm speed.
6	Refrigerant (R290)	130 g gas charged	–	Its ODP value is zero while its GWP value is very low, making it environmentally friendly.
7	Capillary tube	–	1	Compatible with R290 refrigerant
8	Condensate pan	12600 cm^3	1	Made of aluminum sheet material.
9	Overflow pan	900 cm^3	1	Made of aluminum sheet material.
10	Electric resistance (PTC)	350 W	1	Cartridge type resistance.
11	Water pump	48 W	1	It has a 5-meter total delivery head with 0.60 MPa pressure.
12	Ultrasonic humidifier	500 ml/h	1	The water tank is made of silver ion antimicrobial material to keep the steam clean.
13	Antibacterial fabrics	160 x 140 mm	16	They have high dehumidification capacity, fast drying, and high strength.
14	Cold room	1 m^3	–	Isolated from external conditions.

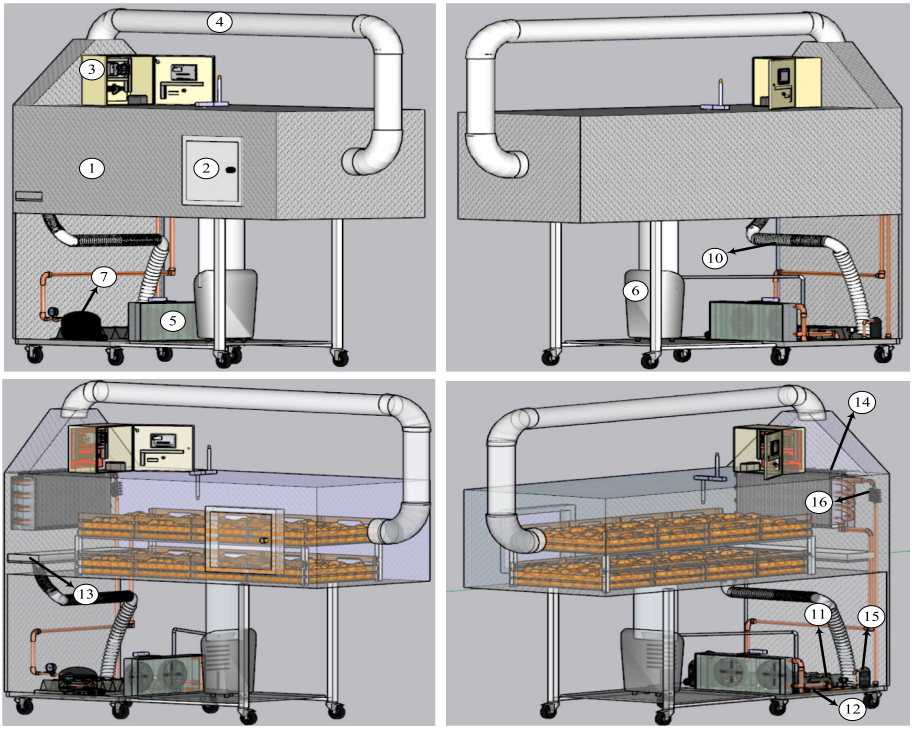

Fig. 2. Modeling view of design. (1: cold room, 2: cold room door, 3: automation panel, 4: evaporator outlet/cold room inlet airline, 5: condenser, 6: ultrasonic humidifier, 7: compressor, 8: cold room temperature relative humidity sensor, 9: evaporator, 10: defrost water drain hose, 11: condensate pan, 12: PTC on overflow pan, 13: defrost water collecting pan, 14: evaporator fans, 15: dryer, 16: capillary tube).

following pages and Table 6.

The schematic Log P-h diagram of the designed refrigeration system is presented in Fig. 3. According to the drawing in Fig. 4; between points 1–2, the compressor compresses the refrigerant and consumes energy, between points 2–2′, energy transfer takes place from the compressor discharge line to the condensate pan, between points 2–3, heat is discharged from the condenser to the environment, between points 3–4, the throttling process takes place through the capillary tube and between points 4–1, the evaporator performs the refrigeration process by extracting heat from the environment.

In this study, a hermetic piston compressor, frequently preferred in refrigeration systems, is used as the basic component of the designed refrigeration system. A micro-channel structure, which is favored in energy-efficient designs with characteristics like low air pressure loss and high heat transfer capacity, is employed for the condenser. An aluminum fin evaporator is utilized due to its high thermal conductivity, durable corrosion resistance, low maintenance, and lightweight structure. A capillary tube that is compatible with R290 refrigerant is also utilized. The system's refrigerant is one of the most important components in the eco-design process and environmental sensitivities. In this context, R290, which has zero ozone depletion potential (ODP) and very low global warming potential (GWP), was used in the designed system. In addition, R290 is also preferred due to its thermodynamically high volumetric heat transfer capacity and environmentally friendly properties. R290 is a pure hydrocarbon and is considered a natural refrigerant. R290 stands out due to its minimal environmental impact, boasting a GWP100yr value of 0.02 per the Intergovernmental Panel on Climate Change AR6 report. R290 has a low viscosity and a higher thermal conductivity in the vapor phase. This leads to the superior performance of R290 in the vapor and two-phase sections of heat exchangers in refrigeration systems. In general, R290 systems show higher COP, reduced refrigerant charge, and lower discharge temperatures than alternatives. However, their heating and refrigeration capacities are lower and require larger compressors. The standard boiling point and critical temperature of R290 are −42.114 °C and 96.74 °C, respectively, which is suitable to ensure a condensing temperature of less than 80 °C at low ambient temperatures. The refrigerant charge of air-source heat pumps using R290 is limited according to international standards, and the discharge temperature and pressure of R290 compressors are lower than those of hydrofluorocarbon and hydrochlorofluorocarbon compressors. However, R290, which is known for its flammability, raises safety concerns in enclosed spaces. R290 refrigerant carries a high flammability risk. Strict adherence to safety protocols and regulations is essential to reduce the potential risks associated with R290 flammability. R290 is generally compatible with various metal alloys and sealants. However, caution should be exercised with materials such as ethylene propylene diene monomer rubber, silicone, and natural rubbers. Refrigerant charging is crucial to ensure that systems comply with safety regulations and achieve optimum system performance. Determining a reasonable charge for each R290 system of different sizes is essential. Considering the hazard of R290, it is necessary to adopt a small system using a special compressor for R290, design the power junction box and control device to ensure complete sealing, and comply with the safety specification during the design, manufacturing, transportation, installation, and use stages [57,58,59].

Based on the emphasis on sustainability, an eco-friendly R290 refrigerant was used in the study, which has an ODP value of zero and a GWP value of 3. In addition, R290 is a popular and prominent refrigerant with strong thermodynamic properties that enable efficient refrigeration and high coefficient performance from the system. Apart from that, the refrigerant has a charge limit due to its high flammability, and in this study, less than 150 g of R290 was charged into the system (130 g). In the study, using this refrigerant with strong thermodynamic properties contributed to the system's energy consumption reduction. With an innovative condensate pan design and water reuse, the desired results were achieved within all the study objectives. All the equipment used in the designed refrigeration system is presented in Table 4 with their specifications.

In the design, the evaporator, with its fans and capillary tube, is in the upper part of the setup. In contrast, the compressor, condenser and its fans, condensate pan, overflow pan in the electric resistance, ultrasonic humidifier, and dryer are in the lower part of the set-up. In defrosting mode, water from a pan beneath the evaporator that is created when snow melts on its surface enters the condensate pan via a drainage line. The pipe system transfers the air at the evaporator outlet to the cold room, which is 200 x 84 x 60 cm in size, 1 m^3 in volume, and isolated from outdoor conditions. Furthermore, an ultrasonic humidifier keeps the products at the desired relative humidity values while in the cold room, and the moisture is transferred to the cold room. In addition, the cold room is designed so that no deterioration is caused by the condensation of water vapor. After the finalization of the design, the experimental set-up is manufactured in Gazi University Energy Systems Engineering Laboratories, Ankara, Türkiye. Fig. 4 presents photographs of the production process and 3D images of the refrigeration system.

After the refrigeration system manufacturing process was completed, the relevant sensors were placed at the different locations shown in Fig. 5. Nine negative temperature coefficient (NTC) sensors, which are placed on copper pipes, three temperature and relative humidity (T/RH) sensors, and one water sensor are used in the system. In addition, current, system voltage, system pressure, air velocity, and mass flow measurements are made from different points of the system. Measurement equipment is given in Table 5.

During the experiments, temperature, relative humidity, pressure, current, voltage, flow rate, frequency, and air velocity values are measured and recorded. These measurements can be affected by errors caused by the reader, the structure of the fasteners, errors caused by the connection points, and the reliability of the measuring device. Therefore, uncertainty analysis needs to be performed to determine the

Table 5
Features of the measurement equipment used in the refrigeration system.

Equipment	Features			
Temperature sensor	Type	Accuracy	Resistance value at 25 °C	Operating temperature range
	NTC	±0.1 °C	10 KΩ ± 1 %	−30 °C to + 105 °C
Thermohygrometer	Temperature range	Temperature accuracy	Relative humidity	Relative humidity accuracy
	−20 to 55 °C	±0.4 °C	0 to 100 %	±2%
Water sensor	Product dimensions	Reading area	Working voltage	Working current
	65x20x8 mm	40x16 mm	5 V	<20 mA
Thermal anemometer	Temperature range	Temperature accuracy	Velocity range	Velocity accuracy
	−20 to 80 °C	±0.1 °C	0 to 20 m/s	±0.03 m/s
Voltage and current sensor	Voltage range	Voltage accuracy	Current range	Current accuracy
	0 to 50 V	±0.1 %	0 to 200 A	±0.4 %
Digital manifold	Temperature range	Temperature accuracy	Operating pressure range	Pressure accuracy
	−55 ℃ to + 125 ℃	±0.5 ℃	−0.1 to 5.0 MPa	±0.4 %
Flowmeter	Measurement range	Mass flow accuracy	Ambient temperature range	Enclosure Rating
	0–1000 kg/h	±0.1 %	−20 °C to + 50 °C	IP 67

Table 6
Experimental procedure.

Test days	Mode-1 PTC + Hot air	Mode-2 Water pump + Ultrasonic humidifier	Cold room set temperature conditions Cold room set relative humidity conditions	Description
Day-1	✓	×	+2 °C / +4 °C% 100	Throughout the experiment, the humidifier was set to 100 % set point, testing extreme conditions to determine the amount of defrost water entering the condensate pan and its removal without overflowing into the environment. The condensate pan was filled to its full volume of 12.6 kg of water. A total of 0.85 kg of water spilled from this pan into the overflow pan before experiment is starting.
Day-2	✓	×	+2 °C / +4 °C 90–95 %	During the experiment, the control algorithm was run according to 90–95 % relative humidity, which is the adequate humidification amount of the products, to save energy in the refrigeration system. At the beginning of the experiment, the condensate pan was filled with up to 12 kg of water. From this pan, 0.35 kg of water was poured into the overflow pan before experiment is starting.
Day-3	×	✓	+2 °C / +4 °C 90–95 %	Instead of the PTC resistance, which consumes a lot of energy in the refrigeration system, a water pump was piped to the overflow pan, and all the water was completely removed by the water pump to be used in the ultrasonic humidifier. Throughout the experiment, the relative humidity of the cold room was kept in the range of 90–95 %, which is sufficient for the food products. The condensate pan was filled to its full volume of 12.6 kg of water. A total of 0.85 kg of water spilled from this pan into the overflow pan before the experiment is starting.
Day-4	×	✓	+2 °C / +4 °C 100 %	The water pump connected to the overflow pan completely removed the defrost water for use in the humidifier, even when the humidifier is operated at 100 % set point. At the beginning of the experiment, the condensate pan was filled with up to 12 kg of water. From this pan, 0.35 kg of water was poured into the overflow pan before experiment is starting.

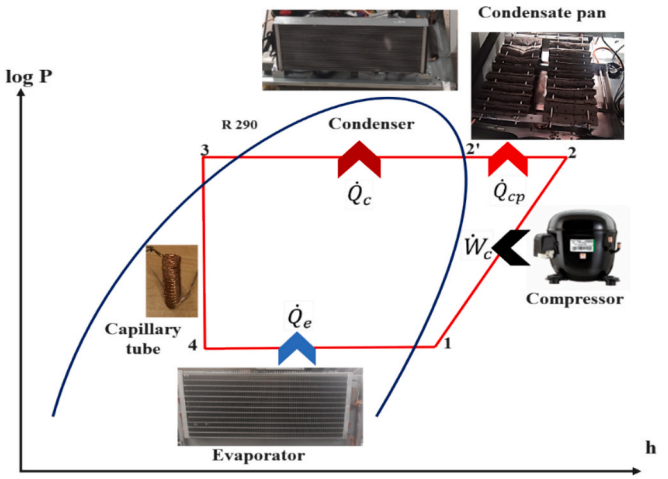

Fig. 3. Log P-h diagram of the refrigeration system.

accuracy of the measurement results. The measuring instruments used were determined according to the characteristics, such as readability, accuracy, and stability, that a measuring instrument should have. The measurement range of the measuring device and the operating temperature were taken into consideration. Increasing the reliability of the experimental results with high-precision equipment was taken into consideration. By applying these criteria, it was aimed to reduce the uncertainties and increase the reliability of the experiments and accordingly, selections were made.

Uncertainty analysis was performed using Eq. (24) on the accuracy values of the equipment given in Table 5. Calculations are made according to errors originating from reading, connection elements, and points, and accuracy-related errors. The uncertainty values are calculated as ± 1.78 % for COP, ±0.65 % for electrical energy consumption value, ±0.14 % for temperature measurement, ±0.51 % for pressure measurement, and ± 0.05 m/s for air velocity measurement. It is determined that the findings obtained were within an acceptable range of uncertainty values and in terms of the reliability of the measurements.

The outputs of all sensors are collected in a central data logger. The information contained in the control unit can be easily accessed. The values obtained serve to determine the permissible operating ranges of the components in the system and enable researchers to conduct in-depth analyses. Optimizing the energy efficiency process in the control algorithm is one of the most significant benefits of using sensors efficiently. Furthermore, using sensors and automation is also crucial for refrigerated products' freshness and food quality.

The experiments are planned to defrost the refrigeration process for

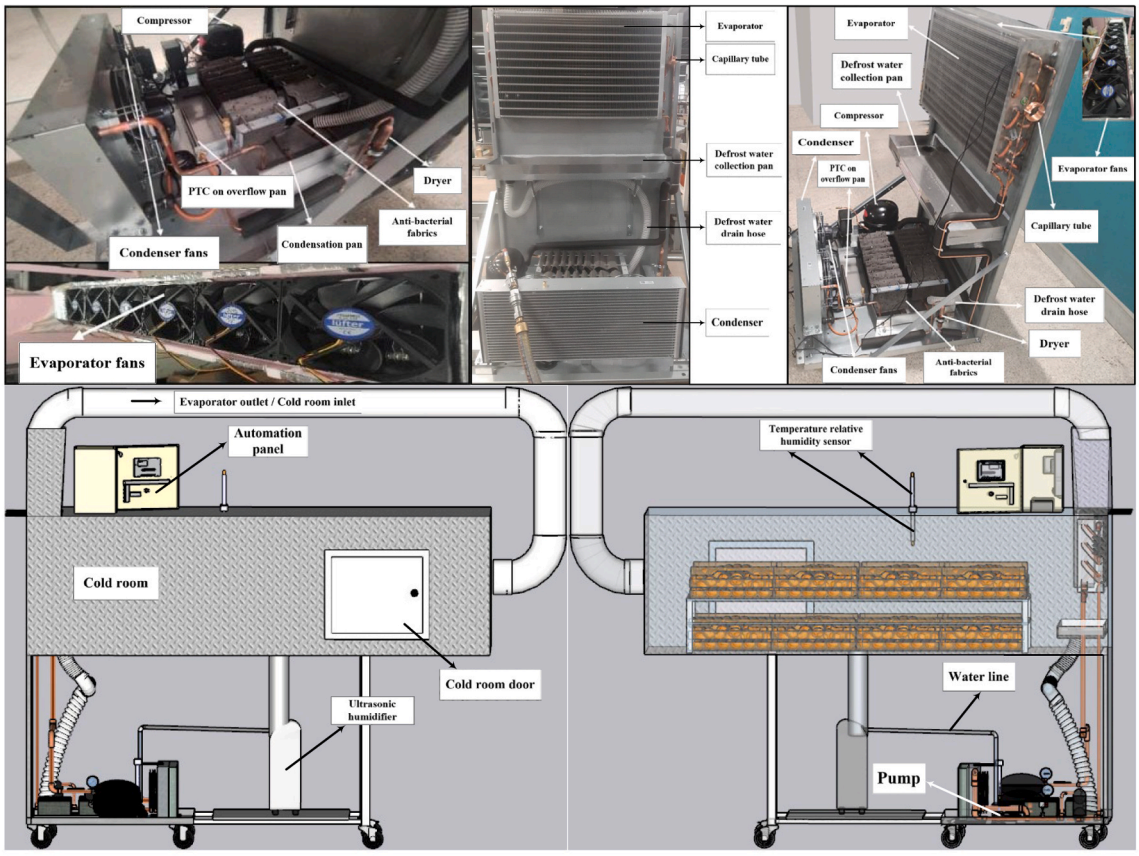

Fig. 4. Various pictures during the production of the refrigeration system and 3D images.

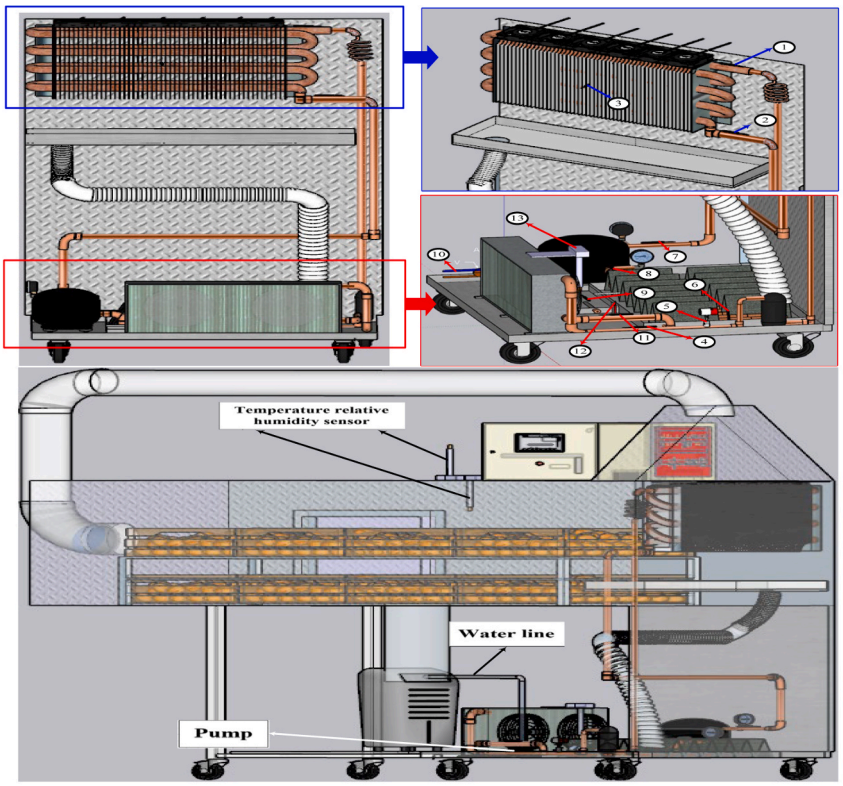

Fig. 5. Sensor locations (1–2–3–4–6–7–8–9–11: temperature sensor, 5: Flow meter, 10: Voltage and current sensor, 12: water level sensor, 13: temperature relative humidity sensor).

15 min after a 3-hour refrigeration process to prevent frost formation on the evaporator and the resulting decrease in efficiency in the system. The defrosting period may vary within the control algorithm according to the data obtained from the relevant sensors. The working structure of the control algorithm and the resulting system behaviors are explained in detail in the next section. Where drain hoses, drip trays, or evaporation chambers are installed, they have sufficient capacity and are designed to be easily accessible and clean. The predetermined climate conditions are ready after the products are placed in the cold room. In addition, the external surfaces of all equipment in the refrigeration unit are wiped dry with a clean cloth before starting the tests. After all these preparations are completed, the experiments are started, and the test period begins.

3.2. Control algorithm

To ensure that the refrigeration process occurs properly and that the system components can operate effectively and efficiently, the system is managed with a control algorithm designed in response to the requirements. Fig. 6 shows the basic circuit diagram of the refrigeration system's control unit. The flow diagram, designed to provide this control, is shown in Fig. 7.

The system is managed according to a three-hour refrigeration mode followed by a 15-minute defrost mode. While deciding the duration of the refrigeration cycle and defrost cycle, heat and mass transfer calculations are carried out by considering the boundary conditions in the direction of the evaporator's air inlet and outlet properties. In the analysis, it is calculated that at the end of 3 h in the refrigeration cycle, the evaporator surface snowed up to 6 mm, and this situation did not reduce the heat transfer coefficient performance of the system. As a result of more refrigeration time, it is determined that the amount of snow on the evaporator surface significantly reduces the heat transfer coefficient. This leads to a decrease in the system's efficiency, and thus, effective refrigeration isn't achieved. In addition, to remove the snowing on the evaporator surface during the refrigeration cycle, it is determined that a defrost time of 15 min is necessary and sufficient.

In both modes, the evaporator fans and the condenser fans operate continuously. In refrigeration mode, the system compressor operates according to the temperature data from the cold room. Accordingly, when the cold room temperature reaches + 4 °C, the compressor is activated, and when the temperature reaches + 2 °C, the compressor is deactivated. In defrost mode, the compressor does not operate. The ultrasonic humidifier, which plays an important role in maintaining the water content of the food products, is activated when the relative humidity in the cold room drops below 90 % and deactivated when this value exceeds 95 %. In defrost mode, the ultrasonic humidifier does not operate. The PTC or water pump in the overflow pan is activated depending on whether there is water in the pan or not. One of the two components continues to operate until the water in the overflow pan is completely depleted. These set points determined in the refrigeration system are designed in such a way that they can be changed instantaneously in line with changing needs.

For the control algorithm to work correctly, sensors are added to various refrigeration system parts. The data obtained from these sensors integrated into the system is collected on a data logger with two cards, which allows 20 different quantities to be measured. The data measured by the sensors are recorded on secure digital (SD) cards every minute. In this context, instantaneous data can be obtained from 20 different points in the refrigeration system. Fig. 8 shows the measured magnitudes and the positioning of the refrigeration system's sensors in the data logger's channels.

3.3. Experimental procedure

As mentioned before, due to the absence of a drainage system in plug-in refrigerators, manufacturers and end users experience various problems in removing the water that occurs during defrosting without overflowing into the environment where the refrigerator is located. Although this situation is currently trying to be solved using PTC resistance, it causes high energy consumption. In addition, relative humidity is a crucial parameter for ensuring product safety while refrigerating foodstuffs. If there is not enough humidification, various deformations may occur in the products, and in cases where humidification is more than necessary, the system consumes unnecessary energy, and frosting increases. To eliminate these negativities, the system is tested in different modes. The experimental procedure of this study, which is conducted on four different days in two different modes, is given in Table 6.

The duration of each test was 6.5 h in total, consisting of two refrigeration and two defrost cycles. When determining the duration of the experiment, it is requested to observe two cycles of each type consecutively. The main purpose of this requirement is to verify, through observation and the data obtained, that the system's behavior in each refrigeration and defrost cycle is consistent. On the first and second days, the defrost water was removed with the help of PTC resistance and hot air. On the third and fourth days of the experiments, named Mode-2, the defrost water was used in the ultrasonic humidifier with the help of a water pump. For both modes, the humidifier was operated at set points of 100 % and 90–95 %.

In the study, humidity ranges were determined based on two considerations. The first consideration is the situation where maximum condensate water occurs. In this case, the 100 % relative humidity condition, called "Extreme RH" in the study, was determined to determine whether there would be an overflow in the system. The second is the 90–95 % RH condition, called "Optimum RH" in the study, which offers the most ideal conditions for storing tangerines in terms of food quality, flavor, and appearance. During the Mode-1 experiments, the ultrasonic humidifier was actively used. During the Mode-2 experiments, the water used in the ultrasonic humidifier is directed to the humidifier through a water line, while in Mode-1, the water reservoir of

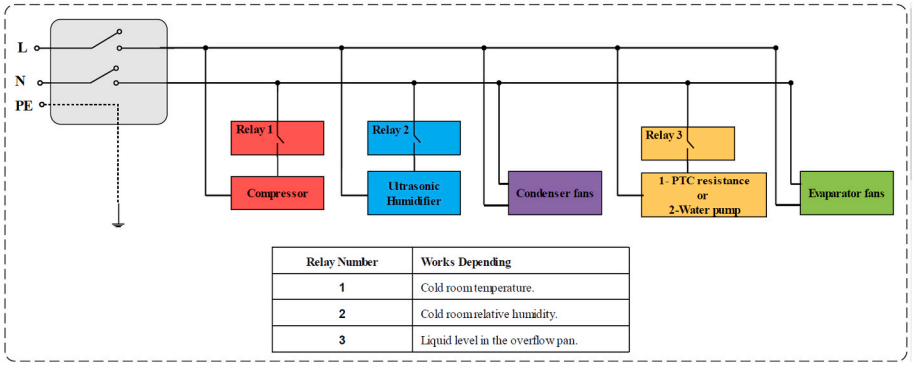

Relay Number	Works Depending
1	Cold room temperature.
2	Cold room relative humidity.
3	Liquid level in the overflow pan.

Fig. 6. Circuit diagram of the refrigeration system.

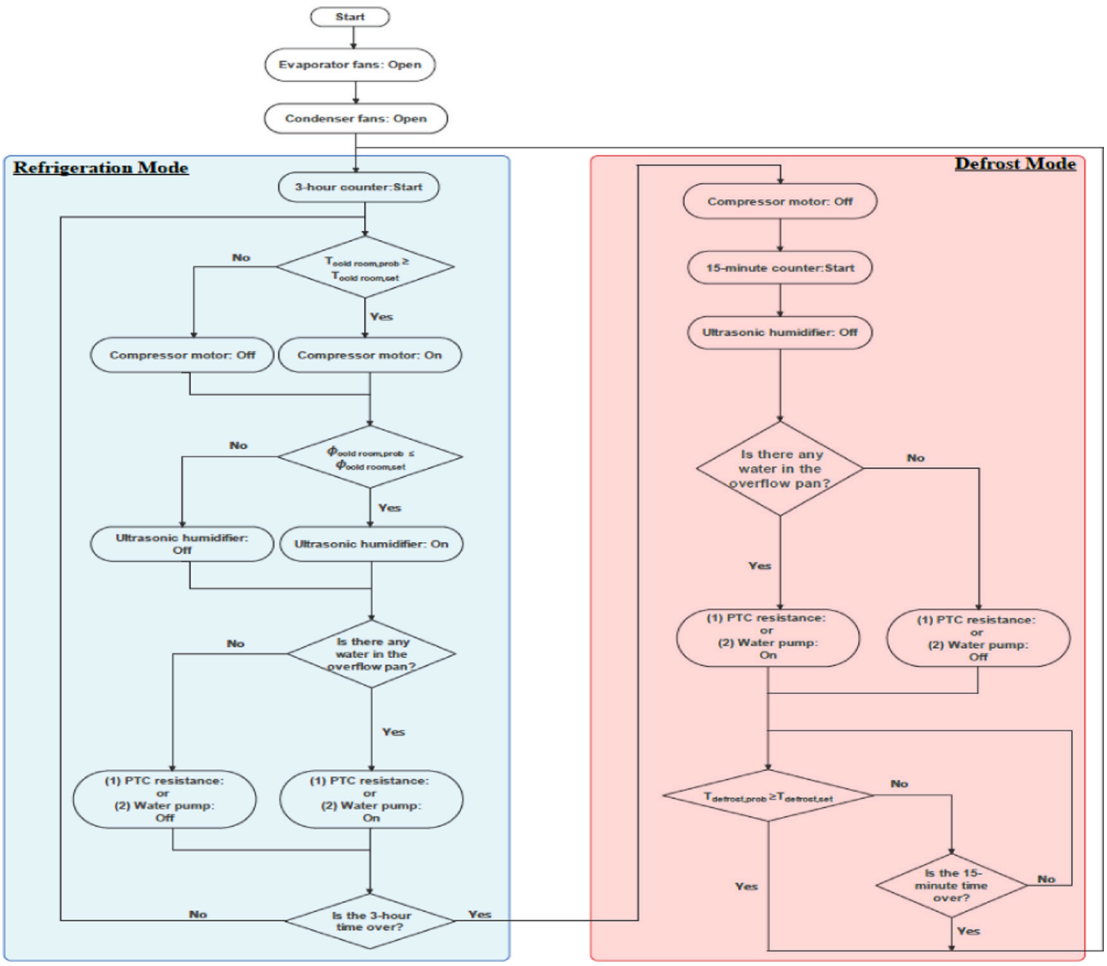

Fig. 7. Control algorithm of the refrigeration system.

the ultrasonic humidifier is manually monitored. When the water in the ultrasonic humidifier is low, water is added to the water reservoir.

When determining the relative humidity level of the cold room, the 100 % relative humidity condition was first determined, which would put the most challenging condition on the system and cause the most amount of water to enter the overflow pan. Secondly, the optimum relative humidity range of 90–95 % was determined for the food product in cold room conditions. Before the experiments in Mode-1 and Mode-2 started, the water tank of the ultrasonic humidifier was filled. During Mode-1 experiments, water was added as the water in the humidifier decreased. During the Mode-2 experiments, the condensate water was reused, and water was added to the ultrasonic humidifier through the water line created by this loop. Also, before the experiments, 30 kg of mandarins, using 6 cases of 5 kg each, were placed in the cold room through the 'cold room door' shown in Fig. 4. In addition, the use of an ultrasonic humidifier in the cold room increased the system refrigeration load.

The data logger unit measured and recorded each test's values. The collected values were analyzed, and the outputs obtained are given in the next section.

4. Results and Discussion

The study's main objective is to rationally remove the defrost water that occurs in plug-in refrigerators in the shortest possible time and most efficiently and effectively. In this way, the refrigerator's energy consumption is reduced, and carbon emissions to the environment are reduced, contributing to global sustainability and reducing the risk of end users paying a carbon tax. With all these, it was aimed to bring an environmentally friendly plug-in refrigerator with improved performance, preferable due to its economic performance, to the sector. In this part of the study, the experiments' results were analyzed, and the outputs and their graphs were presented and interpreted.

In the experiments, the energy consumption data of the systems were analyzed on a component basis. The energy consumption values of the system during 6.5 h of operation, two refrigeration and two defrosting cycles. The comparative graph of the energy consumption of the refrigeration system is presented in Fig. 9, and the graphs of the ratios of the shares of the system components in the total energy consumption during Mode-1 and Mode-2 are presented in Figs. 10 and 11, respectively.

When energy consumption graphs were examined, in Mode-2 experiments, removing defrost water by transferring it to the ultrasonic humidifier using a water pump instead of using PTC created a significant energy saving in the refrigeration system. In this sense, analyzing the data of Day-1 and Day-4, a 29.52 % reduction in total energy consumption has been achieved when the ultrasonic humidifier operated at full capacity. On Day-2 and Day-3, when the relative humidity was kept in the range of 90–95 %, the reduction of energy consumption was 14.35 %.

When the PTC's electrical energy consumption was examined, this component's energy consumption on Day-1 was almost three times higher than on Day-2. This is because the humidifier was operating at full capacity on Day-1, which resulted in more water coming in at defrost time and filling the overflow container with more water. The relative humidity conditions of the cold room also affected the amount

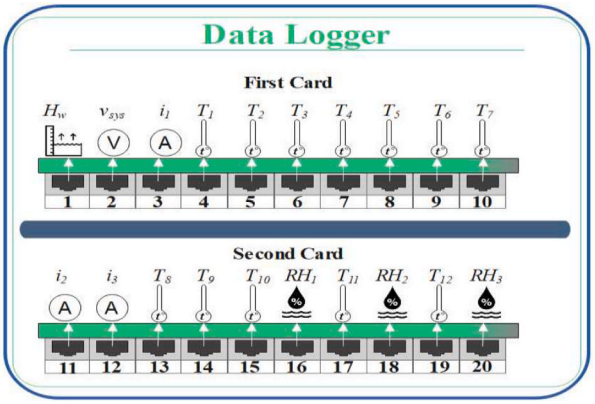

First SD Card		
Measurement point	Measured magnitude	Measurement symbol
1	Water level	H_w
2	System voltage	$v_{sys.}$
3	System total current	i_1
4	Evaporator inlet temperature	T_1
5	Evaporator outlet temperature	T_2
6	Evaporator surface temperature	T_3
7	Compressor discharge (pan inlet) temperature	T_4
8	Compressor suction temperature	T_5
9	Condenser inlet temperature	T_6
10	Condenser outlet temperature	T_7
Second SD Card		
Measurement point	Measured magnitude	Measurement symbol
11	PTC resistance current	i_2
12	Compressor motor current	i_3
13	PTC (overflow) pan water temperature	T_8
14	Condensate pan water temperature	T_9
15	Condenser outlet air temperature	T_{10}
16	Condenser outlet air relative humidity	RH_1
17	Cold room air temperature	T_{11}
18	Cold room air relative humidity	RH_2
19	Outside air temperature	T_{12}
20	Outside air relative humidity	RH_3

Fig. 8. The measured magnitudes and the positioning of the sensors in the data logger's channels.

of energy consumed by the compressor. In this context, the compressor consumed about 10 % less energy on Day-2 and Day-3 when the cold room was kept at optimum humidity conditions compared to Day-1 and Day-4.

The annual reduction effect of this reduction on the refrigeration system area is 704.92 kWh/m^2 and 246.00 kWh/m^2, respectively. As the amount of energy consumed by the PTC decreased, the share of the compressor in the total consumption increased. In addition to this saving in energy consumption, another point that should be emphasized is the reuse of defrost water in a reusable form. Therefore, this study is to develop a design that recognizes the importance of water and contributes to sustainability. in this sense, these days when the effects of the "Global Water Problem", another negative outcome of global warming, are felt more intensely day by day.

During the removal of condensate water in Mode-2, the energy consumed by the ultrasonic humidifier and pump duo used instead of PTC under optimum humidity conditions and extreme humidity conditions is 14.65 % and 21.42 % of the energy consumed by PTC under the same conditions, respectively. The energy consumption values depending on the relative humidity conditions for the relevant components directly used in the removal of condensate water are presented in Fig. 12. When Fig. 12 was examined, the energy consumption value required for the removal of defrost water increased with the rise in relative humidity value of the cold room and it is seen that doing this process with PTC increases the energy consumption significantly.

The developed algorithm manages design values such as relative humidity, temperature, and duration. In this system, which has two modes, refrigeration and defrosting, the algorithm counts the required time, switches from refrigeration mode to defrosting mode and pumps the water to the humidifier. As can be seen in Fig. 12, with the use of the algorithm, energy consumption was low in the case of using an ultrasonic humidifier.

In the system, the humidifier was successfully operated according to the extreme and optimum relative humidity conditions within the control algorithm, and the cold room temperature was kept within the desired range. During the experiments, the average temperature and relative humidity values of the cold room were measured as 3.28 °C / 99.16 %, 3.01 °C / 92.41 %, 2.48 °C / 92.87 %, and 2.50 °C / 99.37 %,

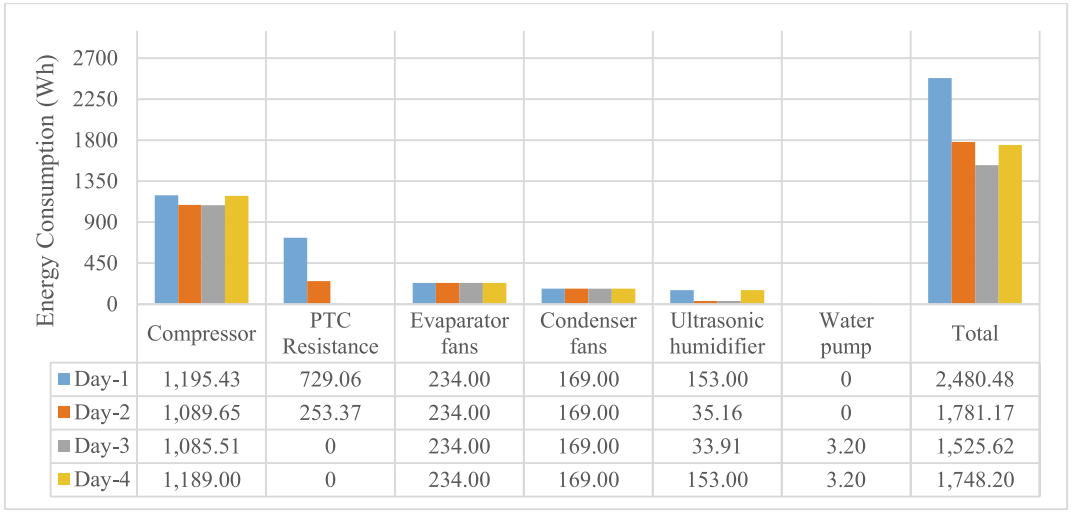

	Compressor	PTC Resistance	Evaporator fans	Condenser fans	Ultrasonic humidifier	Water pump	Total
Day-1	1,195.43	729.06	234.00	169.00	153.00	0	2,480.48
Day-2	1,089.65	253.37	234.00	169.00	35.16	0	1,781.17
Day-3	1,085.51	0	234.00	169.00	33.91	3.20	1,525.62
Day-4	1,189.00	0	234.00	169.00	153.00	3.20	1,748.20

Fig. 9. Total amount of electrical energy consumed in the experiments.

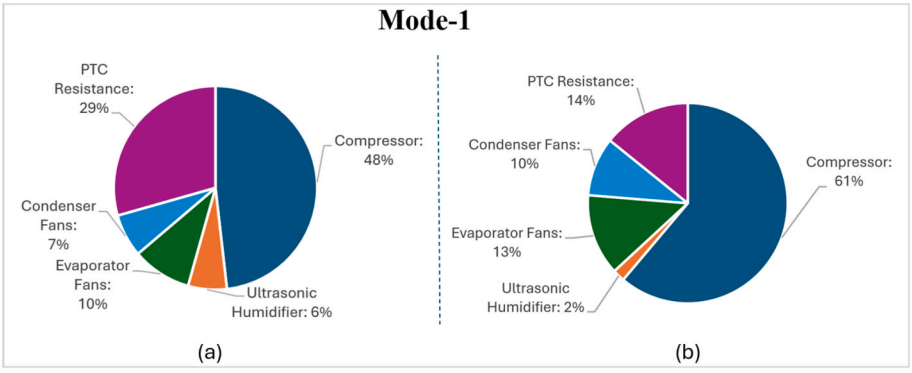

Fig. 10. Component-based energy consumption rates on Mode-1, a) Day-1, b) Day-2.

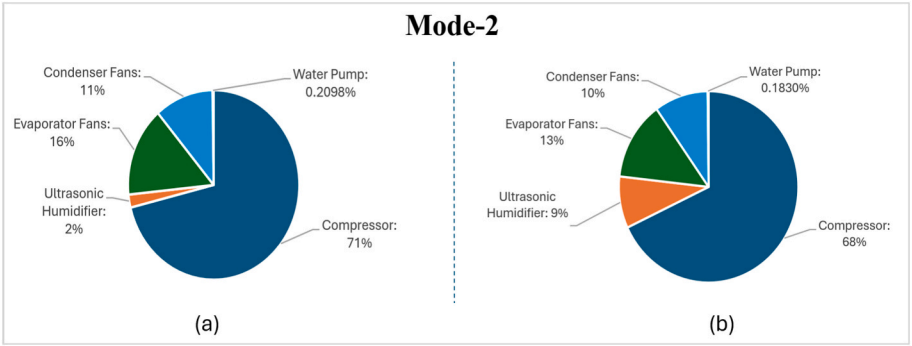

Fig. 11. Component-based energy consumption rates on Mode-2, a) Day-3, b) Day-4.

respectively, daily. These measured values are shown in Fig. 13. When Fig. 13 was examined, it was seen that the cold room operated following the control algorithm, extreme relative humidity conditions increased the refrigeration load and which caused the cold room temperature to rise, and refrigeration was more successful on Day-2 and Day-3. Since refrigeration was provided better in Mode-2 experiments, cold room temperatures were lower than in Mode-1 experiments. In Mode-1 experiments, the average temperature of the cold room was 3.28 °C on Day 1 when the cold room was kept at 100 % relative humidity and 3.01 °C on Day 2 when the cold room was kept at optimum relative humidity. In Mode-2 experiments, the average temperature of the cold room was 2.46 °C on Day 3 when the cold room was kept at optimum relative humidity and 2.49 °C on Day 4 when the cold room was kept at 100 % relative humidity. Due to the higher relative humidity, the cold room temperatures increased slightly on Day 1 and Day 4 compared to the other days in the same mode. In addition, the amount of energy savings achieved by switching from Mode-1 to Mode-2 in the system was 732.28 Wh and 255.55 Wh for the extreme and optimum relative humidity conditions of the cold room, respectively.

As can be seen from the test analysis, PTC resistance had a very significant consumption rate in plug-in refrigeration systems. This component, which was used in both experiments in Mode-1, drew less

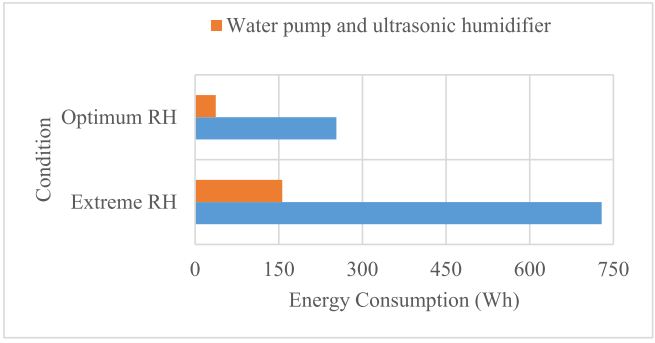

Fig. 12. The energy consumption values depend on the relative humidity conditions for the removal of defrost water.

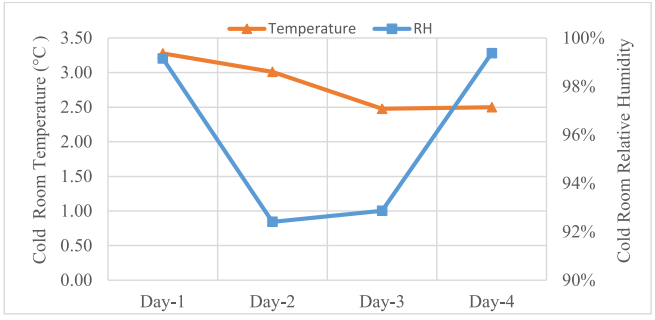

Fig. 13. Cold room temperature and relative humidity values.

current from the grid as the amount of water in the overflow pan decreased. On Day-1, the amount of energy consumed by the PTC is maximum since the experiment was carried out in the most extreme conditions at maximum humidity. When the cold room was controlled with humidity values suitable for the products' storage conditions, the PTC's total electrical energy consumption decreased as the amount of water coming in during defrosting decreased. In Mode-1 experiments, the graph showing the current change of the PTC resistance as a function of water mass was shown in Fig. 14. When Fig. 14 is examined, it is seen that the momentary power of the PTC on Day-1 started with 312.8 W for the maximum water mass and reset at the end of 101 min.

The change for water in the condensate pan and overflow pan on Day-1; during the refrigeration cycle, the overflow pan was depleted entirely of water, reducing the condensate pan by 0.55 kg. During defrosting, 1.37 kg of water flowed from the system into the condensate pan. From there, about 0.83 kg of water was spilled back into the overflow pan. On Day-2, the momentary power of the PTC started at 234.6 W for 0.35 kg of water and resets at the end of 42 min. The change in the amount of water in the condensate pan and overflow pan on Day-2; during the refrigeration cycle, the water in the overflow pan was completely depleted, and 0.50 kg of water was reduced in the condensate pan. During defrosting, 0.86 kg of water flowed from the system into the condensate pan. From there, about 0.32 kg of water was spilled back into the overflow pan. Therefore, the triangle area in the graph is larger on Day-1, which indicates that the PTC resistance consumes more energy.

In the experiments in Mode-1, to remove the water from the overflow pan faster, the condenser fans were placed as close as possible to the pan to ensure that the air hits the water on the pan surface at maximum temperature and velocity and the condenser waste heat was utilized. The theoretical calculations of the time required for the evaporation of water and the experiment's data for the time of complete evaporation are presented in Table 7. When Table 7 was examined, it was observed that the ambient temperature and relative humidity were the same on Day-1 and Day-2, but due to the small amount of water in the overflow panel

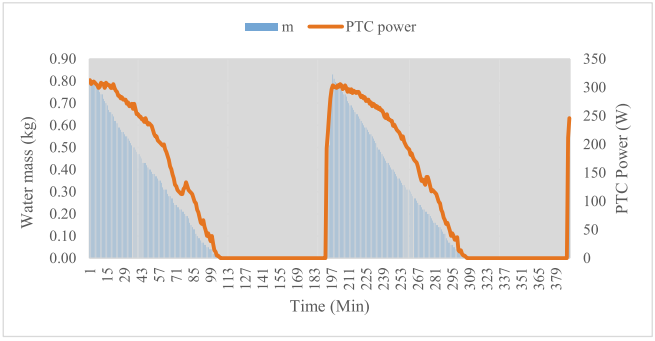

(a) Variation of water mass in the overflow pan on Day-1

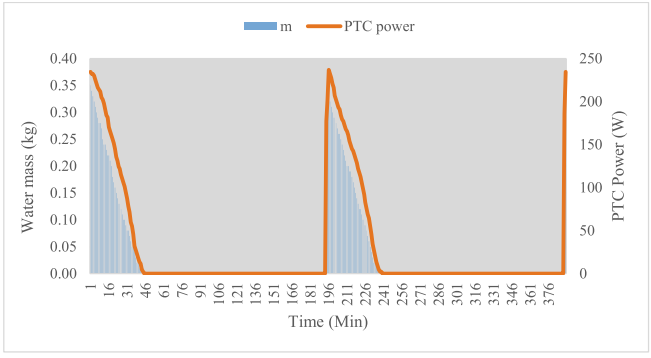

(b) Variation of water mass in the overflow pan on Day-2

Fig. 14. Water mass-dependent PTC power variation during Mode-1 experiments.

Table 7
Required time for the evaporation of water.

Mass Transfer Process	Mode-1 Day-1	Day-2
Air velocity contacts the water on the overflow pan (m/s)	1.50	
Coefficient of mass transfer (m/s)	$1.004x10^{-2}$	
Mass transfer rate of vapor (kg/sm^2)	$1.400x10^{-4}$	$1.489x10^{-4}$
Water mass (kg)	0.81	0.35
Water evaporation time (minute)	96.33	39.17
Realized time in the experiment (minute)	101	42
SMER of evaporated water on overflow pan (kg/kWh)	1.11	1.38

on Day-2, there was a slight difference in the water temperature, which caused 6 % increase in the mass transfer rate of vapor value. In addition, the higher mass transfer rate of vapor value on Day-2 led to a higher SMER value of 0.27 kg/kWh on Day-2 compared to Day-1. The theoretical and experimental values were compatible with each other. The reason for the 5 % increase in time in the experiments is that the air coming out of the condenser fan loses some of its effect on the floor of the pan.

The design aimed to raise the temperature of the water flowing into the overflow pan by allowing the compressor discharge line to pass through the condensate pan and aiding in the evaporation process. In this context, the effect of the change in the condensate pan temperature on the pan efficiency is shown in Fig. 15. When Fig. 15 was examined, as the compressor active time increased, the temperature rise in the discharge line positively affected the pan efficiency. On Day-1 and Day-4, since the ultrasonic humidifier in the system operated at 100 % capacity, the compressor run time increased with the increase in the refrigeration load of the system. On Day-2 and Day-3, the ultrasonic humidifier was kept in the range of 90–95 %, so the compressor run times were less. In this sense, during the three-hour refrigeration cycle,

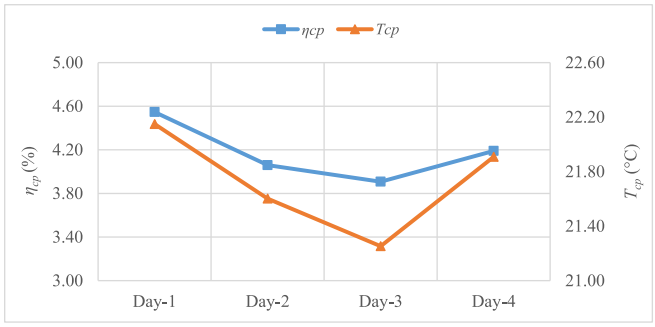

Fig. 15. Condensate pan efficiency.

the compressor was active on average 28 % of the total cycle time on Day-1 and Day-4, 26 % on Day-3 and 25 % on Day-2. As a result, the lowest condensate pan efficiency was observed on Day-3 at 3.90 % and the highest on Day-1 at 4.50 %.

The average measured evaporation and condensation temperatures during the experiments were −7.65 °C / +41.65 °C, −8.66 °C / +40.09 °C, −8.86 °C / +39.02 °C, and −7.64 °C / +40.63 °C, respectively, daily. Experimental average COP and COP Carnot values of the refrigeration system were found to be 2.98 / 5.38, 3.02 / 5.42, 3.10 / 5.52, and 3.08 / 5.50, respectively, daily. The second law efficiency of the system was found to be 55.35 %, 55.73 %, 56.24 %, and 56.03 % respectively, daily. On the first two days, the COP was slightly lower than on the other days because the compressor's isentropic efficiency was lower as the compression ratio of the compressor was higher and the amount of energy consumed in the compressor was higher. The graph of the obtained values is shown in Fig. 16. When Fig. 16 was examined, the second law efficiency was calculated as a result of the exergy destruction values for each test, and the COP values were found to be compatible with each other in the refrigeration system. For all tests, the highest exergy destruction occurred in the compressor and ranged between 50–52 % of the total destruction, while the lowest exergy destruction occurred in the capillary tube and was calculated to be 1 % of the total destruction.

Another focus of this study was an environmentally friendly design approach. As it is known, carbon tax applications have been initiated around the world to prevent the global warming problem. Especially in the production of refrigeration systems, the requirements are developed in a way to shows sensitivity in this direction. Accordingly, eco-friendly R290 refrigerant was preferred in the system design. In addition, the reduction in the system's energy consumption contributed to a more environmental process by affecting the amount of carbon emissions. The carbon emission values for the refrigeration system were calculated as 1,601.26 kg CO_2/year, 1,149.83 kg CO_2/year, 984.86 kg CO_2/year, and 1.128.54 kg CO_2/year, respectively, daily. The environmental-economic results based on carbon emissions were calculated as $23.22/year, $16.67/year, $14.28/year, and $16.36/year, respectively, daily. The annual carbon emissions and related environmental-economic outputs of the refrigeration system on a test basis are shown in Fig. 17. When Fig. 17 was examined, in the Day-1 and Day-4 tests, when the ultrasonic humidifier operates at full capacity, and in the Day-2 and Day-3 tests, when the ultrasonic humidifier operates in the 90–95 % range, the annual reduction effect of carbon emission on the area of the refrigeration system is 337.66 kg CO_2/m^2 and 117.84 kg CO_2/m^2, respectively. With the design of this study, the amount of carbon emission has also decreased due to the decrease in the amount of energy consumption. This has created advantageous results for end users regarding the amount of carbon tax to be paid.

During the design and manufacturing process, it has been acted with the awareness that the earth's resources are limited and that future generations also need these resources. Accordingly, the refrigeration system's depletion and sustainability factor values were calculated as 0.446/2.240, 0.443/2.259, 0.438/2.285, and 0.440/2.274, respectively, daily. When Fig. 18 was examined, as the increase in the system exergy destruction increases the depletion potential, a move away from a sustainable system structure occurred. In this context, it was observed that sustainability and depletion potential contrast with each other and that a more sustainable process occurs at moments of high exergy efficiency during the experiments.

This refrigeration system was designed for commercial use, and its payback period is a valuable indicator of the commercial concerns of end-users. Economic analysis was performed for the optimum RH conditions of the cold room. In this context, when the operating methodology of the system changed from Mode-1 to Mode-2, the payback period was calculated. The energy consumption of the system and the annual profit cost obtained in the enviroeconomic analysis are presented in Table 8.

System costs are very close to each other in Mode-1 and Mode-2 cases. The cost of switching to Mode-2 is $110 in total, including a water pump costing $20, water line labor for $5, and software changing for $75. The costs incurred during the exchange are amortized at the end of the 21st month. In the following years, this cost becomes the system's gain. The amortization period at optimum RH conditions of cold room and the profit obtained by the system are presented in Fig. 19.

In addition, in this study, the performance of the proposed system was compared with the existing refrigeration technologies in literature. It is presented in Table 9. According to Table 9, this study demonstrates a significant improvement in energy efficiency with a 29.52 % energy savings and a COP value of 3.10 for refrigeration systems using R290, compared to other studies in the literature, providing a significant contribution to sustainability and energy efficiency. Specifically, the improvements made offer a solution with high efficiency and environmental benefits for commercial applications, thus establishing this study as an important reference for potential applications in the industry.

In this study, the objectives of minimizing and eliminating the energy

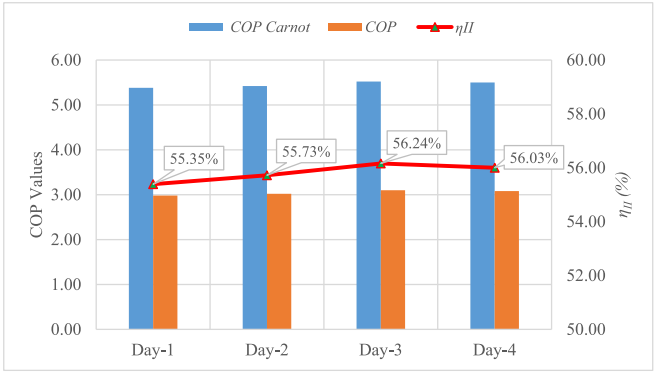

Fig. 16. COP and second law efficiency results.

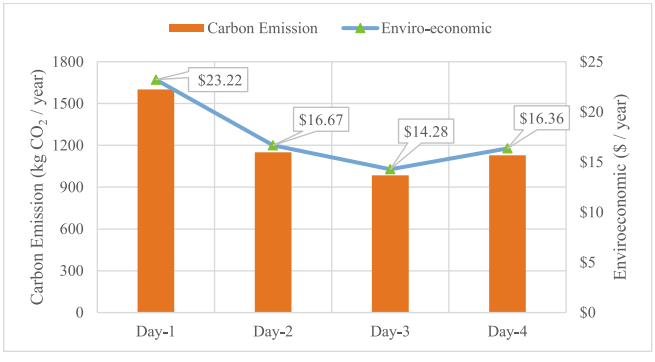

Fig. 17. Carbon emission and enviroeconomic values of the refrigeration system.

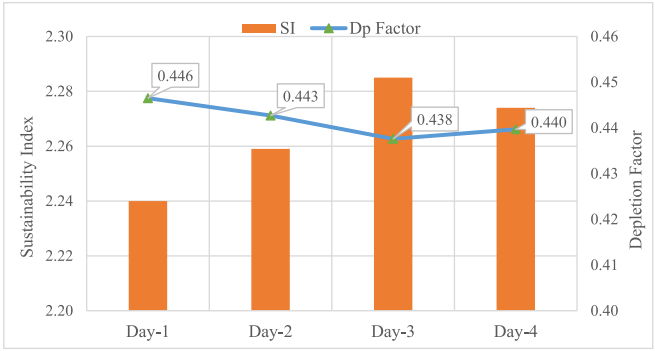

Fig. 18. Depletion factor and sustainability index values of the refrigeration system.

Table 8
Annual profit costs achieved in the refrigeration system.

Condition	In optimum RH
Energy consumption difference profit ($/year)	57.67
Enviroeconomic difference profit ($/year)	2.39
Total profit ($/year)	60.06

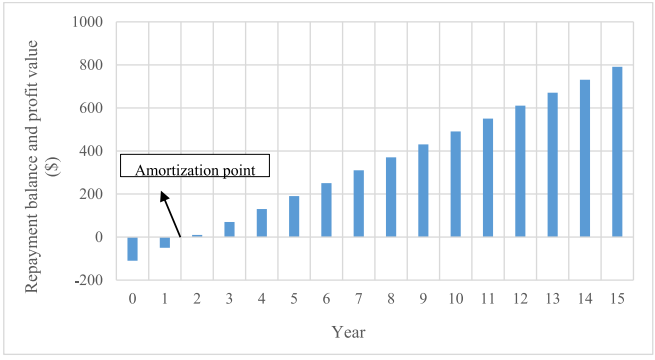

Fig. 19. Amortization period and system profit as a result of the improvements.

consumption due to the condensate consumed by the PTC with the control and automation system were achieved by limiting the energy consumption in Mode-1 and completely eliminating it in Mode-2. It was aimed to prevent the use of PTC, and while the energy consumed by the PTC was 982.43 Wh in Mode-1, this value was reduced to 0 in Mode-2.

There were some limitations in this study, as follows;

- R290 refrigerant with a charge of 130 g was used in this study. In commercial applications, it will be difficult to use R290 due to the maximum charge limit for R290 refrigerant. In these cases, other non-flammable refrigerants may be preferred.
- This study was analyzed for optimum and extreme relative humidity conditions in the cold room. Changing the relative humidity conditions will affect the results obtained.
- In processes where water is reused, it may be necessary to ensure hygiene in the system equipment.

5. Conclusions

This study used low-cost and airflow approaches for commercial-scale manufacturing to construct and test a plug-in refrigeration system using environmentally friendly R290 refrigerant with an inventive condensate pan and humidification unit design. In this study, refrigeration system designs based on original methodologies different from the condensate water removal methods in the literature, which reduce or do not require PTC, were designed, manufactured, tested, and analyzed. With the developed innovative condensate pan, contributions such as decreasing energy consumption during condensate removal, reducing carbon emissions, and increasing sustainability were achieved. In addition, the system also achieved a fast payback period and water savings thanks to the new methodology that reuses condensate water. The obtained values were analyzed for Mode-1 and Mode-2 for optimum and extreme relative humidity conditions in the cold room. The main conclusions of this study were as follows:

- The designed system perfectly met the effective refrigeration requirement of all tests. The best refrigeration performance was provided with a COP value of 3.10 and an exergy efficiency of 56.24 % on Day-3. Moreover, the highest sustainability was achieved on Day-3 with a 2.285 SI value.
- With the switch from Mode-1 to Mode-2, 29.52 % energy efficiency was provided in extreme RH cold room conditions and 14.35 % in optimum RH cold room conditions.
- With the transition from Mode-1 to Mode-2, the payback period for this refrigeration system designed for commercial use was determined as the end of the 21st month at the optimum RH condition.
- Carbon emission values decreased by 337.66 kg CO_2/m^2 per year when the cold room was in extreme RH conditions and 117.84 kg CO_2/m^2 per year when it was in optimum RH conditions. This reduced the annual carbon cost by $6.85/year and $2.39/year, depending on the cold room condition.

Table 9
Comparison of the current study with existing studies in terms of system performance.

Refs.	System Type	COP Value / Improvement Amount
[60]	DX-SAHP (direct expansion solar-assisted heat pump)	The average COP value increased to 2.72. The COP value showed a maximum 32 % increase compared to R134a. Energy efficiency was observed.
[61]	Refrigeration system with R290/R600a mixture using vapor injection	10 % to 20 % higher COP. Maximum COP was achieved with a 40 % R290 mixture by weight. Energy efficiency was observed.
[62]	Optimized VCRS (vapor compression refrigeration system) using R290	Higher COP was achieved with R290 compared to other refrigerants in a system with an evaporation temperature of −3 °C and a condensation temperature of 45 °C.
[63]	R290 cabin heating systems	The COP of the R290 system was 6.7 % to 22.1 % higher compared to conventional systems.
[64]	R290 ASHP (air source heat pump)	COP values were calculated as 2.8 for refrigeration and 3.27 for heating, compared to conventional systems.
[65]	ESRC (ejector subcooling refrigeration cycle)	COP improvements of 17.4 % and 26.6 % were achieved compared to EERC and conventional vapor compression refrigeration cycles.
[66]	R290 air conditioner	Compared to R22, the COP of the R290 window-type air conditioner increased by 2.8 % to 7.9 %, and energy efficiency improvements of 12.4 % to 13.5 % were observed.
[67]	Reconfigured air conditioning system with R290	The COP value increased by 6.5 % when the optimum charge of R290 was between 45–55 % of the full charge amount of R410A. The highest energy efficiency was 21 %.
[68]	R290 cold storage system	The refrigeration COP of the R290 system was on average 1.62 % higher than that of the R134a system at different evaporation temperatures.
This Study	R290 reconfigured refrigeration system	The highest COP value was found to be 3.10 in different modes. A 29.52 % energy savings was achieved as a result of the improvements.

- Defrost water did not overflow into the surrounding environment even when the extreme relative humidity conditions. Thanks to the relative humidity control, the operating time of the PTC is reduced. In fact, with the switch from Mode-1 to Mode-2, there is no need to operate the PTC.

The improvements make this commercial refrigeration system feasible and preferable for end users. The authors predict that a more sustainable and environmentally friendly approach can be created by providing the energy required for the refrigeration system from solar energy in future designs. Energy consumption impacts can be reduced by operating energy consuming equipment, such as fans and compressors with a variable speed control method. The integration of solar energy holds remarkable potential, particularly in expanding the application of low-cost and environmentally friendly refrigeration systems. The incorporation of renewable energy sources in refrigeration systems may have the potential to further reduce energy consumption. The use of solar energy, especially during the summer months, could play a crucial role in meeting the system's energy requirements, thereby providing additional environmental benefits and energy independence.

In addition, it is predicted that energy efficiency will increase further by integrating artificial intelligence into the control system. Artificial intelligence algorithms are anticipated to dynamically manage the refrigeration process according to weather and ambient conditions, enhancing energy efficiency, prolonging the system's lifespan, and airflow management according to the load inside the refrigerating cabinet with the shelf management system. Future work may comprehensively explore the environmental and economic benefits of integrating these technologies. While the initial costs of artificial intelligence integration may be high, considering the long-term energy savings, sustainability benefits, food quality, and shelf life of food processes, it could prove economically advantageous.

Declaration of competing interest

The authors declare that they have no known competing financial interests or personal relationships that could have appeared to influence the work reported in this paper.

Data availability

Data will be made available on request.

References

[1] H. Kauko, K.H. Kvalsvik, N. Masson, C. Noel, S. Minetto, et al., Proposal for the development of the EU ecolabel criteria for food retail stores: preliminary report, Supersmart, (2018) 1-225.

[2] Z. Mylona, M. Kolokotroni, S.A. Tassou, Frozen food retail: Measuring and modelling energy use and space environmental systems in an operational supermarket, Energ. Buildings 144 (2017) 129–143.

[3] J.L. Dupont, The role of refrigeration in the global economy: informatory note, 38th Note on Refrigeration Technologies, Paris, 2019.

[4] M. Orlandi, F.M. Visconi, S. Zampini, CFD assisted design of closed display cabinets, 2nd IIR International Conference on Sustainability and the Cold Chain, Paris, France (2013).

[5] F.W. Yu, K.T. Chan, Optimizing condenser fan control for air-cooled centrifugal chillers, Int. J. Therm. Sci. 47 (2008) 942–953.

[6] K.M. Tsamos, H. Mroue, J. Sun, S.A. Tassou, N. Nicholls, G. Smith, Energy savings potential in using cold-shelves innovation for multi-deck open front refrigerated cabinets, Energy Procedia 161 (2019) 292–299.

[7] C. Ocak, M. Koşan, S. Erten, F.N. Erdoğmuş, M. Öder, Comparison of different compressor technologies for refrigerated display cabinet: Experimental study, Mater. Today Proc. 81 (1) (2023) 74–80.

[8] P.A. Patil, Performance analysis of HFC-404A vapor compression refrigeration system using shell and U-tube smooth and micro-fin tube condensers, A J. Therm. Energy Generation, Transport, Storage, and Conversion 25 (2) (2012) 77–91.

[9] H. Demirpolat, The energy efficiency and environmental analysis of open-type commercial display cabinet with a multi-flow air curtain design, Sustainable Energy Technol. Assess. 60 (2023) 103555.

[10] S. Karyeyen, M. Aktaş, A. Okur, F.N. Erdoğmuş, Numerical analysis of air flow in an industrial refrigeration system and its effect on energy consumption, Gazi Univ. J. Sci. 36 (3) (2023) 1259–1275.

[11] J. Cirera, J.A. Carino, D. Zurita, J.A. Ortega, Improving the energy efficiency of industrial refrigeration systems by means of data-driven load management, Processes 8 (9) (2020) 1106.

[12] Y. Güven, A. Aktaş, M. Aktaş, S. Erten, M. Öder, An example of remote monitoring for a refrigerated display cabinet: effects on energy performance, Gazi Univ. J. Sci. 37 (4) (2024) 1838–1851.

[13] M. Koşan, Y. Dilber, S. Erten, E.M. Bahar, F.N. Erdoğmuş, M. Aktaş, M. Öder, Investigation of the effects of fan control technique on energy consumption in industrial refrigerated display cabinet: An experimental study, Proc. Inst. Mech. Eng., Part E: J. Process Mech. Eng. 238 (1) (2022) 227–239.

[14] S. Thiessen, F.T. Knabben, C. Melo, J.M. Goncalves, An experimental study on the use of vaccum insulation panels in household refrigerators, International Refrigeration and Air Conditioning Conference, Purdue, (2016) 1585.

[15] N.A. Shaban, I. Nasser, J. Al Asfar, S. Al-Qawabah, A.N. Olimat, Thermodynamic and economic analysis of a refrigerator display cabinet equipped with a DC compressor and electronic expansion valve, Int. J. Heat Technol. 38 (2) (2020) 432–438.

[16] D. Rauss, S. Mitchell, R. Faramarzi, Cool retrofit solutions in refrigerated display cases, ACEEE Summer Study on Energy Efficiency in Buildings, Washington, DC, USA, 2008, pp. 233–244.

[17] H. Jouhara, T. Nannou, H. Ghazal, R. Kayyali, S.A. Tassou, S. Lester, Temperature and energy performance of open refrigerated display cabinets using heat pipe shelves, Energy Procedia 123 (2017) 273–280.

[18] Z. Deniz, M. Aktaş, S. Erten, F.N. Erdoğmuş, M. Öder, Analysis of waste heat recovery with finned pipe design in condensate pan for RDCs: effects on energy efficiency, Int. J. Innovative Eng. Appl. 7 (1) (2023) 52–61.

[19] J.A. Evans, A.M. Foster, Sustainable retail refrigeration, John Wiley & Sons Ltd, USA, 2015.

[20] M. Song, G. Xie, L. Pekař, N. Mao, M. Qu, A modeling study on the revere cycle defrosting of an air source heat pump with the melted frost downwards flowing away and local drainage, Energ. Buildings 226 (2017) 110257.

[21] M.A. Rahman, A.M. Jacobi, Drainage of frost melt water from vertical brass surfaces with parallel microgrooves, Int. J. Heat Mass Transf. 55 (2012) 1596–1605.

[22] D. Li, C. Qian, S. Gao, X. Zhao, Y. Zhou, Self-propelled drop jumping during defrosting and drainage characteristic of frost melt water from inclined superhydrophobic surface, Int. J. Refrig 79 (2017) 25–38.

[23] M.H. Kim, H. Kim, D.R. Kim, K.S. Lee, A novel louvered fin design to enhance thermal and drainage performances during periodic frosting/defrosting conditions, Energ. Conver. Manage. 110 (2016) 494–500.

[24] P.K. Bansal, G. Xie, A simulation model for evaporation of defrosted water in household refrigerators, Int. J. Refrig 22 (4) (1999) 319–333.

[25] Q. Zhou, H. Wang, S. Liu, H. Wei, G. Hu, Assessment of the heat transfer efficiency of perforated louvered fins for improved drainage, Int. J. Heat Mass Transf. 228 (2024) 125654.

[26] M.A. Delele, A. Schenk, E. Tijskens, H. Ramon, B.M. Nicolaï, P. Verboven, Optimization of the humidification of cold stores by pressurized water atomizers based on a multiscale CFD model, J. Food Eng. 91 (2) (2009) 228–239.

[27] S. Fabbri, S.I. Olsen, M. Owsianiak, Improving environmental performance of post-harvest supply chains of fruits and vegetables in Europe: Potential contribution from ultrasonic humidification, J. Clean. Prod. 182 (2018) 16–26.

[28] T. Brown, J.E. Corry, J.A. Evans, Humidification of unwrapped chilled meat on retail display using an ultrasonic fogging system, Meat Sci. 77 (4) (2007) 670–677.

[29] D. Tirawat, D. Flick, V. Mérendet, E. Derens, O. Laguerre, Combination of fogging and refrigeration for white asparagus preservation on vegetable stalls, Postharvest Biol. Technol. 124 (2017) 8–17.

[30] S. Jhee, K.S. Lee, Defrosting behavior of fin-tube heat exchanger with PTC heating sheet, Int. J. Air-Conditioning and Refrig. 9 (1) (2001) 29–38.

[31] J. Westhaeuser, H. Schatz, J.C. Albrecht, W. Tegethoff, N. Lemke, J. Koehler, Analysis of cyclic frosting and defrosting of a vehicle heat pump, Int. J. Refrig 152 (2023) 241–255.

[32] A. Steiner, R. Rieberer, Simulation based identification of the ideal defrost start time for a heat pump system for electric vehicles, Int. J. Refrig 57 (2015) 87–93.

[33] M. Wang, X. Jiang, Y. Chen, T. Li, Q. Chen, L. Ma, Development and application of the low Curie point positive temperature coefficient (PTC) electrothermal anti-icing material, Polymer 291 (2024) 126601.

[34] İ. Dinçer, Thermodynamics: A smart approach, Wiley, 2021, p. 463.

[35] P. Giménez-Prades, J. Navarro-Esbrí, C.M. Udroiu, A. Mota-Babiloni, Influence of subcooling in R-449A supermarket refrigeration system and screening of refrigerant mixtures for its energetic and environmental improvement, Appl. Therm. Eng. 236 (2024) 121787.

[36] İ. Dinçer, Refrigeration systems and applications, Wiley, 2003, p. 162.

[37] R. Yamankaradeniz, İ. Horuz, S. Coşkun, Ö. Kaynaklı, N. Yamankaradeniz, Refrigeration technology and heat pump applications (Fourth Edition), Dora Publications, 2021, pp. 31–33.

[38] B. Aktekeli, M. Aktaş, M. Koşan, Y. Güven, E. Arslan, Experimental investigation of a new defrosting technique for sustainable refrigeration system, Therm. Sci. Eng. Prog. 54 (2024) 102849.

[39] Y. Xu, A. Tula, X. Chen, Integrated product selection and process optimization for cascade refrigeration system, Int. J. Refrig 156 (2023) 173–185.

[40] Y. Wang, Y. Zheng, X. Hu, S. Liu, X. Li, Q. Wang, Impact of condensate water recycling on the performance of open refrigerated display cabinet, Case Stud. Therm. Eng. 54 (2024) 104022.

[41] Y.A. Çengel, Heat and mass transfer (Third edition), Güven Publishing, 2011, pp. 811–813.
[42] Y.A. Çengel, A.J. Gahjar, Heat and mass transfer fundamentals and applications (Fourth edition), McGraw-Hill, 2011, pp. 717–784.
[43] S.J. Babalis, E. Papanicolau, N. Kyriakis, V.G. Belessiotis, Evaluation of thin-layer drying models for describing drying kinetics of figs (Ficus carica), J. Food Eng. 75 (2) (2006) 205–214.
[44] F. Bayrak, M. Aktaş, A. Aktaş, S. Şevik, B. Aktekeli, Y. Güven, Analysis of a novel PVT dryer using a sustainable control approach, Renew. Energy 245 (2025) 122728.
[45] H. Çalışkan, Novel approaches to exergy and economy based enhanced environmental analyses for energy systems, Energ. Conver. Manage. 89 (2015) 156–161.
[46] A. Ustaoğlu, B. Kurşuncu, A.M. Kayan, H. Çalışkan, Analysis of vapor compression refrigeration cycle using advanced exergetic approach with Taguchi and ANOVA optimization and refrigerant selection with enviroeconomic concerns by TOPSIS analysis, Sustain. Energy Technol. Assess. 52 (2022) 102182.
[47] C.S. Rajoria, S. Agrawal, G.N. Tiwari, Exergetic and enviroeconomic analysis of novel hybrid PVT array, Sol. Energy 88 (2013) 110–119.
[48] A. Shahsavar, P. Talebizadehsardari, M. Arıcı, Comparative energy, exergy, environmental, exergoeconomic, and enviroeconomic analysis of building integrated photovoltaic/thermal, earth-air heat exchanger, and hybrid systems, J. Clean. Prod. 362 (2022) 132510.
[49] ISO 23953-2:2023, Refrigerated display cabinets — Part 2: Classification, requirements and test conditions. International Standards Organization, (2023).
[50] E. Arslan, M. Koşan, M. Aktaş, S. Erten, Experimental assessment of comparative R290 vs. R449A refrigerants by using 3E (energy, exergy and environment) analysis: a supermarket application, J. Therm. Eng. 7 (3) (2021) 595–607.
[51] M.G. Gado, S. Ookawara, S. Nada, H. Hassan, Renewable energy-based cascade adsorption-compression refrigeration system: Energy, exergy, exergoeconomic and enviroeconomic perspectives, Energy 253 (2022) 124127.
[52] M.A. Rosen, İ. Dinçer, M. Kanoğlu, Role of exergy in increasing efficiency and sustainability and reducing environmental impact, Energy Policy 36 (1) (2008) 128–137.
[53] J.P. Holman, Experimental methods for engineers, McGraw-Hill, USA, New York, 1966.
[54] Z. Tietel, E. Lewinsohn, E. Fallik, R. Porat, Importance of storage temperatures in maintaining flavor and quality of mandarins, Postharvest Biol. Technol. 64 (1) (2012) 175–182.
[55] M.C. Strano, G. Altieri, M. Allegra, G.C. Di Renzo, G. Paterna, A. Matera, F. Genovese, Postharvest technologies of fresh citrus fruit: advances and recent developments for the loss reduction during handling and storage, Horticulturae 8 (7) (2022) 612.
[56] L.M. Manolopoulou, P. Papadopoulou, Effect of storage temperature on encore mandarin quality, ISHS Acta Horticulturae 379 (1995) 475–482.
[57] A.A.B. Issa, C. Liang, E.A. Groll, D. Ziviani, Residential heat pump and air conditioning systems with propane (R290) refrigerant: Technology review and future perspectives, Appl. Therm. Eng. 266 (2025) 125560.
[58] Y. Du, J. Wu, C. Wang, Experimental study on dynamic characteristics of an R290 heat pump during defrost, Energ. Buildings 223 (2020) 110174.
[59] Z. Yang, B. Feng, H. Ma, L. Zhang, C. Duan, B. Liu, Y. Zhang, S. Chen, Z. Yang, Analysis of lower GWP and flammable alternative refrigerants, Int. J. Refrig 126 (2021) 12–22.
[60] X. Kong, M. Zhang, Y. Yang, Y. Li, D. Wang, Comparative experimental analysis of direct-expansion solar-assisted heat pump water heaters using R134a and R290, Sol. Energy 203 (2020) 187–196.
[61] M. Özsipahi, H.A. Köse, H. Kerpiççi, H. Güneş, Experimental study of R290/R600a mixtures in vapor compression refrigeration system, Int. J. Refrig 133 (2022) 247–258.
[62] C.H. de Paula, W.M. Duarte, T.T.M. Rocha, R.N. de Oliveira, A.A.T. Maia, Optimal design and environmental, energy and exergy analysis of a vapor compression refrigeration system using R290, R1234yf, and R744 as alternatives to replace R134a, Int. J. Refrig 113 (2020) 10–20.
[63] S. Kwon, D. Lee, J.Y. Chung, H. Maeng, Y. Kim, Performance comparison of a direct heat pump using R1234yf and indirect heat pumps using R1234yf and R290 designed for cabin heating of electric vehicles, Energy 297 (2024) 131311.
[64] W. Tang, G. He, S. Zhou, W. Sun, D. Cai, K. Mei, The performance and risk assessment of R290 in a 13 kW air source heat pump, Appl. Therm. Eng. 144 (2018) 392–402.
[65] Y. Liu, J. Yu, Performance evaluation of an ejector subcooling refrigeration cycle with zeotropic mixture R290/R170 for low-temperature freezer applications, Appl. Therm. Eng. 161 (2019) 114128.
[66] S. Devotta, A.S. Padalkar, N.K. Sane, Performance assessment of HC-290 as a drop-in substitute to HCFC-22 in a window air conditioner, Int. J. Refrig 28 (4) (2005) 594–604.
[67] T.B. Fajar, P.R. Bagas, S. Ukhi, M.I. Alhamid, A. Lubis, Energy and exergy analysis of an R410A small vapor compression system retrofitted with R290, Case Stud. Therm. Eng. 21 (2020) 100671.
[68] H. Zheng, G. Tian, Y. Zhao, C. Jin, F. Ju, C. Wang, Experimental study of R290 replacement R134a in cold storage air conditioning system, Case Stud. Therm. Eng. 36 (2022) 102203.